universität wien

MASTERARBEIT | MASTER'S THESIS

Titel | Title

Reliability of Subject-Specific BOLD Response to Different TMS Protocols in the DLPFC

verfasst von | submitted by

Dominik Zeman

angestrebter akademischer Grad | in partial fulfilment of the requirements for the degree of

Master of Science (MSc)

Wien | Vienna, 2025

Studienkennzahl lt. Studienblatt | Degree programme code as it appears on the student record sheet:	UA 066 013
Studienrichtung lt. Studienblatt | Degree programme as it appears on the student record sheet:	Masterstudium Joint-Degree Middle European interdisc. master prog. in Cognitive Science
Betreut von | Supervisor:	Assoz. Prof. Dipl.-Ing. Dr.techn. Christian Windischberger Privatdoz.

Acknowledgements

I would firstly like to thank my supervisor Christian Windischberger for giving me the opportunity to conduct rigorous work and for his support throughout this process, but most importantly for making the whole genuinely enjoyable.

I would especially like to thank my co-supervisor and scientific mentor Sarah Grosshagauer for all of the help in designing and conducting the experiment for this thesis. Thank you for standing by me and trusting me with conducting the scans from the briefest and easiest to the most challenging ones. Each click of the stimulator made me a better scientist and I cannot thank you enough for inspiring me to seize the opportunities I have worked hard for and helping me grow as a researcher.

I would also like to thank all current and past colleagues from the fMRI, TMS, and MR Physics groups in the MR Center of Excellence at the Medical University of Vienna for all of their efforts and foundational work that has allowed me to conduct this study. A special thanks to all participants of this study for their time and effort in the scanner and under the stimulator.

I would also like to express gratitude to the past head of MEi:CogSci program at the University of Vienna Markus F. Peschl and coordinator Elisabeth Zimmermann for their organization of the study program and their efforts in teaching their classes. I can honestly say that I gained a lot of new knowledge while being engaged and having fun.

A thank you also goes out to my exchange semester supervisor Kristína Malinovská and co-supervisor Tamara Bíla for their project mentorship during my exchange at the Faculty of Mathematics, Physics and Informatics at Comenius University.

I would like to thank my MEi:CogSci classmates for all of the time we spent together inside and outside of the classroom. I would especially like to thank Clara, Harkeerat, and Tobias for always being there to talk to and making this masters so much more fun.

Lastly, I would also like to thank my parents and my brothers for their unwavering support, kind words during stressful times, and their celebrations during times of success. Similarly I want to thank my friends Nela, Michal, Boris, Samuel, Juraj, and all others for being there for me throughout this journey and for the adventures we took around the world during the time of this master's.

I could not have done it without everyone that helped and supported me.

Abstract

Transcranial magnetic stimulation (TMS) is a method used for non-invasive brain stimulation. It is commonly used in research labs for causally investigating specific brain regions' impact on behavior and whole brain activation and in clinics as a intervention method for treatment resistant psychiatric disorders. When combined with functional magnetic resonance imaging (fMRI) the immediate effects of TMS can be observed through the blood oxygen level dependent (BOLD) response at the stimulation site and in its associated brain networks. This method gives researchers the ability to observe the effect of stimulation in real time and causally probe the functionality of specific brain regions. While the within-session reliability of TMS-fMRI has been investigated before, its reliability across different sessions on different days remains unexplored. This research utilizes concurrent TMS-fMRI to investigate the brain activations caused by different stimulation protocols and how consistent they are across sessions, checking for differences within and between subjects, as well as differences in protocols.

For the study we recruited eight healthy participants who partook in three separate scanning sessions on a 3T Siemens PrismaFit MR scanner. The first session conducted was an intake session where eligibility was deemed, and active motor threshold and resting state scans were acquired to develop subject specific electric field guided amplitude adjustment and Dorsolateral Prefrontal Cortex (dlPFC) targeting based on inversely correlated activations to the Subgenual Anterior Cingulate Cortex (sgACC) respectively. The two following concurrent TMS-fMRI sessions were conducted on separate days, separated by at least 24 hours. During each stimulation session two stimulation runs were conducted applying either single pulses or 10 Hz triplets, the order of which reversed from one session to another. Subjects received 30 individual stimulations over an 8.5 minute scan. The functional data was then analyzed on a subject- and group-level. Reliability analysis was conducted by grouping the data into functionally defined parcels across different brain networks. Within- and between-subject similarity was calculated by assessing Pearson's correlation of the parcel-wise effect sizes.

We found that within-subject reliability is higher than between-subject reliability stressing the importance of individualized stimulation procedures during TMS as individual anatomies and functional connectivity differences contribute to significant differences in activations across subjects. In parallel we found the parcel-wise correlation between sessions of triplets to be higher than singlets suggesting that single pulses might not be sufficient to create reliable BOLD in the dlPFC. These effects were found both on a whole-brain and individual-network level. These findings demonstrate that triplets are superior to singlets in the resulting BOLD responses. Overall, this study contributes to a deeper understanding of the mechanics of non-invasive brain stimulation as well as the broader knowledge base of cognitive science by investigating the often assumed stability

of brain networks across time.

Kurzfassung

Die transkranielle Magnetstimulation (TMS) ist eine Methode zur nicht-invasiven Hirnstimulation. Sie wird häufig in der Forschung eingesetzt, um die Funktion bestimmter Hirnregionen zu untersuchen, sowie als Behandlung für therapieresistente psychiatrische Erkrankungen. In Kombination mit der funktionellen Magnetresonanztomographie (fMRT) können die unmittelbaren Auswirkungen der TMS anhand des BOLD-Kontrasts beobachtet werden. So lassen sich sowohl die Wirkung der Stimulation als auch die Rolle bestimmter Hirnareale besser verstehen. Während die Stabilität der BOLD-Antwort innerhalb einer einzelnen TMS-fMRT-Sitzung bereits untersucht wurde, ist wenig darüber bekannt, wie stabil diese Reaktionen über mehrere Tage hinweg sind. In dieser Studie haben wir daher getestet, wie konstant die durch unterschiedliche TMS-Protokolle ausgelösten Hirnaktivierungen über mehrere Sitzungen bleiben und wie stark sie zwischen Proband:innen sowie verschiedenen Stimulationsprotokollen variieren.

Acht gesunde Proband:Innen wurden für diese Studie rekrutiert und nahmen an jeweils drei Messungen teil. Alle Messungen wurden an einem 3T Siemens PrismaFit MR-Scanner durchgeführt. In der ersten Sitzung wurden Ruhezustands-fMRT Messungen aufgenommen sowie der aktive Motorschwellwert bestimmt. Anschließend wurde eine probandenspezifische, durch das elektrische Feld bestimmte Intensität berechnet sowie ein Zielgebiet definiert. Dieses Zielgebiet wurde im linken dorsolateralen präfrontalen Kortex (dlPFC) auf der Grundlage von invers korrelierten Aktivierungen des subgenualen anterioren cingulären Kortex (sgACC) lokalisiert. Die beiden TMS-fMRT-Sitzungen fanden an getrennten Tagen statt. Jede Sitzung umfasste zwei Läufe mit entweder Einzelimpulsen oder 10-Hz-Tripletts, wobei die Reihenfolge zwischen den Sitzungen getauscht wurde. Pro Lauf wurden 30 Stimulationen in 8.5 min verabreicht. Die funktionellen Daten wurden anschließend auf Probanden- und Gruppenebene analysiert. Die Konstanz der Aktivierung über die Sitzungen hinweg wurde in funktionell definierten Hirnnetzwerken mithilfe von Pearson-Korrelationen der jeweiligen Effektgrößen untersucht.

Unsere Ergebnisse zeigen, dass die Aktivierungsmuster innerhalb einer Person relativ stabil sind, sich jedoch stark zwischen verschiedenen Personen unterscheiden. Dies unterstreicht die Bedeutung individuell angepasster Stimulationsstrategien. Zudem zeigte sich, dass die Konsistenz der Aktivierungen zwischen Sitzungen bei Triplett-Stimulation deutlich höher war. Einzelimpulse scheinen hingegen weniger zuverlässige BOLD-Antworten zu erzeugen. Diese Effekte traten sowohl auf Netzwerkebene als auch im gesamten Gehirn auf. Die Ergebnisse zeigen, dass Triplett-Stimulation der Einzelpuls-Stimulation hinsichtlich der resultierenden BOLD-Antwort überlegen ist. Damit liefert diese Studie wichtige Hinweise darauf, wie sich TMS-induzierte Hirnantworten über die Zeit verändern und betonen die Relevanz individueller Unterschiede in der Konnektivität für die resultierende Aktivierung.

Contents

List of Acronyms

aMT Active Motor Threshold. 31

ATP Adenosine Triphosphate. 13

BIDS Brain Imaging Data Structure. 33

BOLD Blood Oxygen Level Dependent. 2

CMRR Center for Magnetic Resonance Research. 40

CSF Cerebrospinal Fluid. 34

dlPFC Dorsolateral Prefrontal Cortex. 10

E-field Electric Field. 5

EEG Electroencephalography. 2

EPI Echo Planar Imaging. 33

fMRI Functional Magnetic Resonance Imaging. 2

FWHM Full Width at Half Maximum. 14

GLM General Linear Model. 36

HRF Hemodynamic Response Function. 14

IR Infra Red. 16

MDD Major Depressive Disorder. 2

MNI Montreal Neurological Institute. 37

MP2RAGE Magnetization Prepared 2 Rapid Gradient Echo. 33

MPRAGE Magnetization Prepared Rapid Gradient Echo. 40

MR Magnetic Resonance. 13

MRI Magnetic Resonance Imaging. 12

MSO Maximum Stimulator Output. 30

NIfTI Neuroimaging Informatics Technology Initiative. 36

NMR Nuclear Magnetic Resonance. 12

OCD Obsessive Compulsive Disorder. 2

PMd Dorsal Premotor Cortex. 19

RF Radio Frequency. 13

ROI Region of Interest. 38

rTMS Repetitive Transcranial Magnetic Stimulation. 2

sgACC Subgenual Anterior Cingulate Cortex. 11

SimNIBS Simulation of Non-Invasive Brain Stimulation. 7

SSRI Selective Serotonin Reuptake Inhibitor. 2

TBS Theta Burst Stimulation. 10

TE Echo Time. 40

TMS Transcranial Magnetic Stimulation. 1

TR Repetition Time. 40

TSE Turbo Spin Echo. 40

WM White Matter. 34

List of Tables

List of Figures

1. Introduction

Colloquially, the phrase "mentally stable" is used to describe someone of sound mind. While this phrase is generally used jokingly and does not have a place in the scientific setting, it begs the question: Are we even mentally stable? Beyond dated and somewhat demeaning terminology used for labeling people with psychiatric disorders, this question represents an idea of cognitive science that is seldom explored. How stable are the ways in which cognition comes to be? Do the organs that we primarily use for cognition have reliable ways of producing said cognition? This study investigates how concurrent transcranial magnetic stimulation and functional magnetic resonance imaging can be used to probe the reliability of the causal and distributed neural dynamics underlying cognition.

The brain plays a central role in cognition. While theories of cognition, such as embodiment, emphasize the role of the whole body [1], the brain and its doings cannot be ignored. As the central processing unit of the body, most of the signals we receive and output as humans pass through the brain. In coming closer to understanding cognition, it is therefore important to understand the brain, as a central mechanism in cognition. The study of the nervous system, formally known as neuroscience, relies on a plethora of different methods which all yield different information about what this complex organ does. Many of these methods depend on passive observation of what the brain is doing while others alter behavior, allowing active interaction with the brain to trigger specific outcomes. These perturbation methods range from simple behavioral tasks to pharmacology, and most relevant for this thesis, brain stimulation.

Brain stimulation is a family of methods that allow doctors and researchers to directly probe and influence the workings of the brain. It is one of the most extensively growing fields of cognitive science and neuroscience as it provides causal insights about the workings of specific anatomically defined brain regions and how they collaborate in large-scale networks. Since stimulation is a powerful tool, significant efforts have been made to make it better. The methods have evolved to be less painful, less invasive, and helpful beyond probing the functionalities of individual cortical brain regions.

Transcranial Magnetic Stimulation, or TMS, is a method that allows for completely non-invasive brain stimulation through indirect current induction in the subject's brain. The technology exploits the basic physical principles of the law of induction to induce an electric field in the cortical tissue, directly underneath the coil, and can therefore trigger neuronal activation in the target site and its associated networks [2]. This technology has allowed researchers to causally probe the workings of the brain. It has proven itself to be a powerful research tool for cognitive science and neuroscience but its implications exceed far beyond these fields.

Most practically, TMS is an incredibly powerful tool for treating psychiatric disorders.

Roughly 5% of humanity suffers from major depressive disorder (MDD) [3]. Of the affected population roughly 30% of patients are classified as treatment resistant [4]. Currently, the most utilized first-line treatment is pharmaceuticals. Through the use of medications such as selective serotonin re-uptake inhibitors (SSRI), patients with psychiatric disorders have been treated successfully. However, for many patients, the standard treatments do not alleviate disease burden or have severe side effects. Because of this, TMS has been a promising treatment method that allows for the modulation of specific brain regions and networks implicated in different disorders. Through repeated transcranial magnetic stimulation (rTMS), disorders such as major depressive disorder (MDD), obsessive compulsive disorder (OCD), and even neurological disorders such as epilepsy have seen new methods of treatment that are much less invasive [5, 6, 7].

Beyond its clinical applications, TMS has provided cognitive science researchers with an incredibly powerful tool for exploring brain function. It allows us to investigate the effects of activation in specific brain regions and what cognitive effects they might have. Other investigation methods, such as direct cortical stimulation, require the opening of the skull, or in the case of simple functional magnetic resonance imaging (fMRI) studies, lack causality and only investigate correlations. TMS provides a causal investigation method by allowing direct induction of activation in a small area of the cortex and observation of the effects. TMS provides a well-validated balance of high spatial focality, minimal invasiveness, and full compatibility with imaging methods such as functional magnetic resonance imaging (fMRI) and electroencephalography (EEG), making it one of the most practical tools for causal perturbation of localized cortical regions. The technology brings us much closer to mapping behavioral and cognitive phenomena onto brain regions.

This thesis investigates the reliability of brain activation as a response to TMS in specific target regions across multiple sessions separated by days to weeks. While previous research has demonstrated that TMS can produce consistent brain activation patterns within a single session [8], the temporal stability of these responses across separate sessions remains largely unexplored. This is a critical gap given that clinical TMS applications for conditions like MDD often rely on repeated stimulation over time. To address this, I utilized concurrent interleaved TMS-fMRI with precise neuronavigation to ensure sub-millimeter targeting accuracy across sessions. By comparing the blood oxygen level dependent (BOLD) response patterns both within the same subject across multiple sessions and between different subjects, and by testing two distinct stimulation protocols, this study aims to quantify the reproducibility of TMS-evoked brain activation and determine whether protocol-specific effects influence response stability. This methodological approach not only tests assumptions about the consistency of brain network dynamics underlying cognition, it also provides crucial empirical data for establishing TMS-fMRI as a predictor of clinical treatment response. This research is fundamentally interdisciplinary from the methodology it utilities to the implications it provides. The methods span medical physics, psychiatry, and cognitive science. Findings from this study have implications towards cognitive science, psychology, and cognitive computational modeling. The principle of reliability is often assumed by researchers and not empirically investigated. This assumption permeates and shapes the way experiments are designed and cognitive

processes modeled. This study utilities causal perturbation to investigate the stability of the central processing unit, which is the brain, providing concrete evidence for the assumptions of various fields and providing a deeper insight into the fundamental ways in which cognitive science research is conducted.

The motivations for a study like this are extensive. The most practical motivation is expanding the understanding of how TMS impacts the brain for the sake of improving psychiatric disorder treatment methodology. Understanding its mechanisms, provides more insights for researchers to focus on making the technology itself better and more accessible, so more patients can utilize it with a higher success rate. This study probes something that is seldom explored in cognitive science literature: the stability of the brain. Our brain is an evolving organ that changes and adapts throughout our lives. With fluctuations of brain activity happening on the scale of seconds to years [9], it begs the question of how reproducible and reliable the activations as a result of a specific stimulus or stimulation at different times are. Very frequently studies focus on single-session effects of a certain stimulus or stimulation, and do not factor in the possibility that there might be differences in response across time. TMS-fMRI studies provide us with an incredibly powerful tool to causally explore how stimulation at a specific site, stimulated with a high degree of precision, impacts the brain on different days. Do the activations follow the same patterns in the same brain or do they change strongly across different days. Is the brain stable in the way it responds to stimuli or are there major variations in brain activation as a result of interaction with external stimuli? Should we expect to see the same activation patterns across different stimulation sessions? Stability of the brain is often assumed by researchers when making claims about the brain's workings. This study aims to explore this essential aspect of cognition.

2. Background

This chapter outlines the theoretical background behind the experiments conducted. It is an overview of transcranial magnetic stimulation, functional magnetic resonance imaging, and the concurrent use of the two technologies. It covers the the basic principles behind the technology, its uses, and their implications towards cognitive science knowledge.

2.1. TMS

Transcranial magnetic stimulation (TMS) is a noninvasive method for modulating brain activity by using rapidly changing magnetic fields to induce electrical currents in targeted cortical regions [2]. It enables researchers to directly influence neuronal activity and observe resulting behavioral or physiological effects, making it a unique tool for establishing causal links between brain function and cognition. Computational modeling techniques further enhance its precision by allowing individualized simulations of how stimulation induces electric field in the brain (E-field), optimizing coil placement and stimulation parameters [10]. TMS is widely regarded as a safe and well-tolerated procedure when proper screening and safety protocols are followed, thereby minimizing potential risks such as seizures or discomfort [11]. Owing to its versatility, TMS is now central to both experimental neuroscience and clinical practice, bridging the gap between fundamental research and therapeutic application.

2.1.1. Technology

TMS is based on the physical principle of induction. First described by Michael Faraday in 1831, induction refers to the phenomenon of a changing magnetic field inducing current in a conductor. This principle applies to all conductors, including neural tissue. As a conductor passes through a homogeneous magnetic field, the free electrons in the material experience the magnetic component of the Lorentz force, causing movement of the free electrons across the material, thereby the induction of an electric field within the material. This simple principle is exploited in the case of transcranial magnetic stimulation shown in Figure 2.1.

The TMS coil is a simple electric circuit consisting of a source of current, a capacitor, a switch, and a figure-of-eight-shaped coil of wire. As the switch is activated, the capacitor releases the stored charge from the power supply, resulting in a brief electric pulse to travel across the coil of wire. As the current is passed through the coil, the coil produces a magnetic field in the direction perpendicular to the coil. The specific shape of the wire defines the shape of the magnetic field produced [13]; figure-of-eight coils are generally

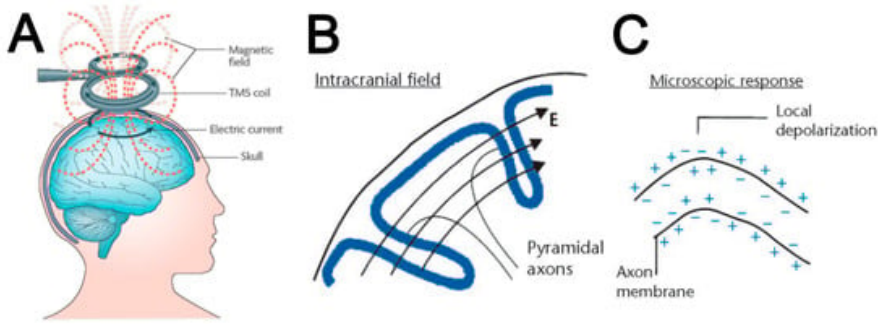

Figure 2.1.: Overview of electromagnetic induction in TMS: (A) A brief pulsed current flows through a coil generating a magnetic field, which passes through the skull and induces a secondary current, which stimulates the brain. (B) The electric field (E) within the brain runs through cortical folia essentially perpendicular to the descending pyramidal neuron axons. (C) Microscopically, the secondary current can locally alter the axon membrane potential and therefore activate neuronal firing. Image and caption acquired from [12], published in the International Journal of Molecular Sciences under the Creative Commons Attribution (CC BY) license.

used due to the focality of the E-field produced as a result of stimulation in the brain. Impact of coil geometry on shape of electric field produced is shown in Figure 2.2.

The magnetic field produced by the coil, when the coil is placed on a person's head, passes through the skull and soft tissue and reaches the brain. The true effects of stimulation on neurons are an active area of research. Barker and colleagues discovered that stimulating the motor cortex using TMS causes neural activation localized in the brain region directly under the coil [2]. When stimulating the primary motor area, the researchers were able to elicit a motor response in the form of hand movement in the contra lateral arm. Due to the limited penetration depth of TMS, the crowns of the gyri are the most impacted by stimulation [15]. On a neuronal level, the site where the action potential originates is likely the myelinated axon terminals of pyramidal cells and inhibitory inter-neurons [15], though the true effects of TMS on neurons and their substructures is still being investigated. Activation of these local neuronal populations sums to form population-level currents, which in turn recruit circuits and activity in connected pathways. As a result, TMS-induced effects are not confined to the stimulation site but can propagate along axons and synapses to functionally connected regions of the brain. This hierarchical spread from local neuronal excitation to network-level modulation is what makes TMS a powerful method for the causal investigation of brain function in targeted regions of interest.

Using modeling and simulation, it has become possible to simulate the induced E-field in the brain. This allows for tracing physically induced stimulation patterns, but does not allow to directly simulate brain response. The tissues of the head have specific conductive properties, which allows us to model exactly how stimulation causes electric

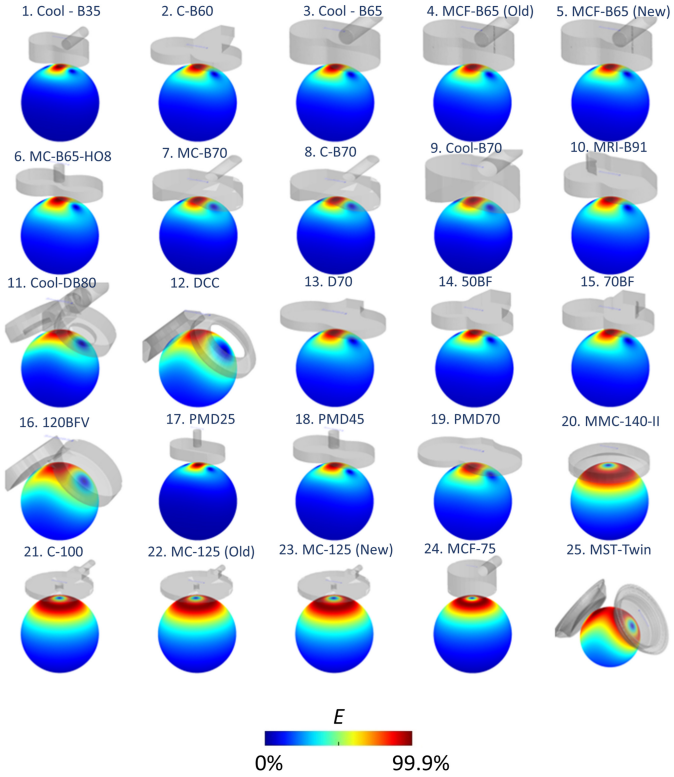

Figure 2.2.: Induced electric field distribution of 25 TMS coils. The simulations were conducted with SimNIBS software. The coil cases were created in Blender (https://www.blender.org/). All coils were placed at the center of the sphere head with directions as seen at the figure. Image and caption acquired from [14], published in Brain Stimulation under the Creative Commons Attribution (CC BY) license.

field propagation at each point in the cortex. For this, researchers utilise simulation software, one of them being SimNIBS. SimNIBS is an open-source software for modeling of non-invasive brain stimulation [10]. The software works by segmenting the head into 15 different tissues [16]. The different types of tissues in the brain and head have varying conductivities and are prone to conducting the induced electric field at different rates [17]. This allows researchers to create personalized head models of subjects and customize the optimal coil positions and rotations for specific target stimulation and adjust the stimulation intensity required to reach an adequate amount of E-field in the target regions [18] (this method is elaborated in Section 3.4.5).

2.1.2. Safety

TMS is broadly regarded as a safe and well-tolerated noninvasive brain stimulation technique when established safety protocols are followed. It has received regulatory

approval for both research and clinical use from bodies such as the U.S. Food and Drug Administration (FDA) and the European CE certification [19]. Nevertheless, several contraindications and precautions must be carefully considered to ensure participant safety. While the instance rate of seizures is extremely low, the primary risk associated with TMS is seizures, particularly in individuals with conditions or medications that lower the seizure threshold [11]. Those with epilepsy, a family history of seizure disorders, or the users of psychoactive drugs such as antidepressants, antipsychotics, or stimulants should be screened thoroughly, as these factors may heighten susceptibility to TMS-induced seizures [11]. Additional safety considerations span the presence of metallic or electronic implants such as pacemakers, cochlear implants, deep-brain stimulators, and other neural prostheses which could be displaced, heated, or disabled by the magnetic field [11]. Even superficial materials, including iron oxide-based tattoo pigments, metal-containing cosmetics, or piercings near the stimulation site, can cause local heating or irritation and should be removed or evaluated before stimulation [11]. Accurate coil positioning and minimization of subject movement are also essential, as excessive movement can compromise targeting precision. Because of this, live neuronavigation is recommended. Auditory safety is yet another key concern, as the coil discharge produces a loud noise that can be heard through both air and bone conduction, potentially worsening conditions such as tinnitus. Hearing protection, typically in the form of earplugs, is therefore standard practice. While TMS has not been shown to produce adverse effects in pregnant individuals or children, the lack of long-term safety data urges a conservative approach that generally excludes these populations [11].

2.1.3. Example Applications in Cognitive Science

TMS, as a method in cognitive science research, has been a key development in recent years, allowing researchers to directly and causally probe the functionality of specific brain regions. Its impact is quite substantial because cognitive science methods often rely on correlative relationships during investigation, to limit the impact of the method on the subject as a whole. TMS has allowed the scientific community to observe the impacts of activation and inhibition of localized brain areas and networks, which has in turn brought us closer to understanding their functional role in the context of network-level activation and behavior. It has most prominently been used for language, learning, working memory, and brain plasticity studies, but there are many areas of study where TMS can provide valuable insights in the future.

Language

Language is an almost uniquely human cognitive ability that has been thoroughly investigated using TMS. It is a task that involves multiple brain regions and allows us to communicate complex concepts to other humans. Language abilities are key to everyday life and therefore careful steps need to be taken during brain surgery to avoid permanent changes to the person's speech abilities. For this, the Wada test is most utilized to assess to which side of the brain the speech center is lateralized. The test temporarily inhibits

one hemisphere of the brain by injecting a barbiturate into the corresponding internal carotid artery [20]. While that side is inactive, doctors test the patient's language and memory abilities to determine which hemisphere controls these functions before brain surgery. This test is, however, highly invasive and poses risks to the participant. Repetitive TMS allows for noninvasive, reversible, and precise mapping of language function through the inhibition of specific brain regions. In one of the first cognitive TMS studies by Epstein and colleagues, rTMS over the left posterior-inferior frontal region reliably induced speech arrest while sparing other language functions such as comprehension, naming, and writing [21]. The results of this study correlate with the results of the Wada test in epileptic patients and therefore provide a different, less invasive method for lateralizing speech production functions. Newer studies have used speech arrest on tumor patients demonstrating functional reorganization of the brain by language functionalities shifting from left to right hemisphere after a tumor affects language regions [22]. Similarly, a recent study using time-specific inhibitory double-pulse TMS over the left inferior frontal gyrus and left posterior middle temporal gyrus demonstrated that disrupting these regions at critical moments selectively disrupts gesture–speech semantic integration, showing their causal and time-dependent contributions to multi-modal language processing [23]. In another study, researchers found that the opposite effect to speech arrest can also be reached through TMS. Stimulating Wernicke's area significantly reduced naming latencies when applied half a second to a second before stimulus presentation [24]. This effect occurred only at moderate stimulation intensities, suggesting that TMS can pre-activate language-related neural networks to enhance language processing. The combination of these studies allows researchers to precisely map language regions in the brain by functionality, giving surgeons new methods of localizing, and greatly decreasing chances of negative side effects post-surgery.

Learning and Working Memory

Working memory is a limited-capacity system responsible for the temporary storage and manipulation of information necessary for cognitive tasks. This ability allows us to store important pieces of information while doing tasks such as cooking using a recipe or holding a phone number in memory before dialing it. In an early application of TMS to motor learning, researchers used a serial reaction time task for studying implicit motor sequence learning. Participants performed a repeating motor sequence, and as they learned it, their reaction times decreased due to anticipation of upcoming movements. Notably, cortical motor maps of the involved finger muscles expanded during this learning phase, but only until participants consciously recognized the sequence pattern [25]. Once explicit knowledge of the sequence was achieved, the cortical expansion disappeared despite continued performance improvements, indicating that control, previously processed by the primary motor cortex, had shifted to higher-order networks. This study demonstrated the value of TMS as a mapping tool capable of tracking dynamic changes in cortical organization during learning. TMS can be employed not merely as a readout method but as an active working memory modulation technique. Postle and colleagues first used fMRI to identify brain regions involved in working memory manipulation versus simple

retention. They then applied repetitive TMS (rTMS) to dlPFC and superior parietal lobule while participants performed tasks requiring either short-term retention alone or retention plus manipulation of information. The researchers found that disrupting dlPFC activity with rTMS during the delay period impaired performance on tasks requiring manipulation but not on tasks requiring only retention of the same information. Critically, this effect was specific to prefrontal cortex as disruption of parietal regions affected both retention and manipulation [26].

Neuroplasticity

In recent years, the term neuroplasticity has been popularized and its implications have been stretched beyond our actual understanding of what it is and how it occurs. Brain plasticity is the brain's ability to change its structure and function in response to experience, learning, or injury. It involves the strengthening, weakening, or formation of new neural connections, allowing the brain to adapt to new demands or recover lost functions. TMS has been a powerful tool of not only inducing neuroplasticity but also investigating the ways in which plasticity happens in the brain. In an experiment looking at more short-term plasticity, Classen and colleagues used TMS by utilizing the finger twitch response [27]. Subjects were stimulated to elicit a thumb movement in a specific direction. Afterwards, subjects practiced the movement in the opposite direction. After practicing, when stimulation occurred in the same site as before, the elicited movement was in the practiced direction, not the original direction [27]. This finding suggests that the same neural architecture shows short-term plasticity to induce different motion outcomes based on learning and experience. More long-term plasticity options have been explored as well. Huang and colleagues have developed a rTMS protocol named theta burst stimulation (TBS) which has been shown to consistently induce long-lasting effects on motor cortex physiology beyond the time of active stimulation [28]. In a recent review, TBS-TMS protocols have been assessed and have been shown to make long lasting changes in specific brain regions and networks [29]. Pharmacological work has shown that both long-term potentiation and depression of TBS depend on specific receptor mechanisms, indicating that these protocols induce synaptic plasticity in the human motor cortex. One of the biggest advantages of TMS as a tool is that repetitive application of stimulation has the ability to make lasting changes to the functional organization of the brain. Beyond investigating cognitive phenomena, this has been the biggest factor enabling clinicians to use the technology as a disorder intervention. Thus, TMS has shown itself to be helpful in research labs as well as clinics.

2.1.4. Clinical Applications

Beyond research, TMS has been established as a treatment modality for various psychiatric and neurological disorders. Since the method can target specific brain regions, it provides a much more personalized treatment compared to the most common current pharmacological treatment approaches. Therefore, TMS is currently being explored for the treatment for major depressive disorder, obsessive compulsive disorder, epilepsy, and many other

psychiatric or neurological disorders. Thus far it has proven itself to be an effective treatment method that has been shown to provide symptom relief in patient cohorts which are considered treatment resistant to standard interventions such as pharmacological treatments.

Major Depressive Disorder

The most common clinical application for TMS is treatment-resistant major depressive disorder. Major depressive disorder is characterized as a psychiatric disorder with a multitude of symptoms such as persistent depressed mood, suicidal ideation, insomnia, and others [30]. According to the World Health Organisation's reports, it is estimated that roughly 5% of the world's population suffers from this disorder [3]. The first-line treatment for MDD are selective serotonin re-uptake inhibitors (SSRI). This class of pharmaceuticals functions by limiting the uptake of serotonin from the synaptic cleft, increasing the concentration of serotonin in the synaptic cleft. This form of treatment is, however, nowhere near perfect and reports show that roughly 30% of patients are classified as treatment resistant [4]. Treatment resistant patients are those who utilize various treatment methods with limited results. For these patients, TMS is often the last line of battle against their psychiatric disorders. The repetitive application of TMS was initially pioneered in the 1990s and showed that the technology can be used to alleviate symptoms of depression in clinically diagnosed patients [31]. Since then, large strides have been made to further understand the effects and improve the results of this treatment. The technology works on the basis of locally modulating activation in areas and networks responsible for the symptoms of depression. The subgenual anterior cingulate cortex (sgACC) is a deep brain area whose dysfunction has been linked with symptoms of depression [32]. Since it is a deep brain region, however, it cannot be directly stimulated by TMS, as TMS is only able to stimulate superficial cortical areas. The sgACC, however, can be modulated using stimulation in the dlPFC [33] as the two areas have an inverse firing functional connectivity [34]. Increasing activity in the sgACC, e.g. through neuromodulation with TMS, allows for the brain to adjust through neuroplasticity, increasing the baseline activation in the area, improving the symptoms of depression. Thus, TMS has been used in depression treatments in patients previously considered treatment resistant and has been reported to have significant remission rates of symptoms in patients [5]. Because of its efficacy, the technology has been used in treatment worldwide, with advancements in treatment outcome being improved as the technology improves.

Obsessive Compulsive Disorder

Obsessive-compulsive disorder (OCD) is a psychiatric disorder characterized by the prevalence of unwanted, recurrent, and persistent thoughts that lead to compulsive mental or physical acts with rigid rules [30]. This is a debilitating mental health disorder that largely impacts a persons' ability to lead everyday lives through impulsive, often repetitive behaviors over which the persons have little to no control. Patients with a

treatment-resistant form of OCD may find TMS to be a worthy treatment option if classical pharmacological treatments do not incite remission of symptoms. An early study on the stimulation of parts of the prefrontal cortex has been shown to alleviate compulsive thoughts and other symptoms immediately after treatment and lasting for several hours [6]. Review studies of short and long-term clinical trials using TMS to treat OCD indicate a 22.7% improvement in symptoms [35] placing it among other effective treatment methods. With developments in technology, treatment methods, and accessibility TMS is on route to be used in treatment for many other disorders besides MDD and OCD.

Epilepsy

The treatment implications of TMS are not only confined to psychiatric disorders but also overlap with neurological diseases. Epilepsy is a disorder defined by spontaneous chronic seizures. During an epileptic seizure, the brain activity is highly excessive rhythmic activity across the entire brain [36]. Interestingly enough, although epilepsy or a family history of epilepsy is generally an exclusion criterion in TMS studies, there have been very recent attempts at treating the disorder using non-invasive stimulation. TMS can not only produce an excitatory effect in the brain but has also been attributed inhibitory effects, allowing to decrease activation, decreasing activation in personalized target brain regions. With its ability to down-regulate brain activity, TMS has been shown to significantly decrease seizure rate in epileptic patients with a reduction of 72% to 78.9% per week [7]. TMS as a treatment for epilepsy is currently only conducted on very few patients with forms of epilepsy that are resistant to pharmacological treatments and still needs to be thoroughly explored. Still it is a promising method for alleviating disease burden in epilepsy patients.

2.2. fMRI

In terms of non-invasive brain imaging methods, Magnetic resonance imaging is the state-of-the-art technology currently used in the field. The method provides high spatial resolution of whole-brain activation patterns which cannot be seen through any other imaging modality without the use of invasive substances or ionising radiation.

2.2.1. Magnetic Resonance Imaging

Magnetic resonance imaging, or MRI for short, is a method of imaging objects, in most cases tissue, based on the principle of nuclear magnetic resonance (NMR) [37]. Nuclear magnetic resonance (NMR) exploits a quantum mechanical property of protons which is referred to as spin. A thorough explanation of NMR, the basic principle behind MRI, is beyond the scope of the thesis. The following is a bare-bones explanation of the basic principles behind this imaging method. Importantly, MRI typically focuses on the proton in the nucleus of a hydrogen atom, which shows high natural abundance in different tissue types. When placed in a strong static magnetic field, these spins align with the field, and the application of radiofrequency pulses temporarily disturbs this alignment

[38]. As the spins relax back to equilibrium, they emit measurable radiofrequency (RF) energy that can be detected with RF coils and spatially localized using magnetic field gradients [38]. These signals are then reconstructed into images that reflect differences in tissue composition. In functional MRI, these signals provide the basis for detecting hemodynamic changes linked to neural activation talked about in Section 2.2.3, allowing researchers to infer patterns of brain activity.

2.2.2. Functional Magnetic Resonance Imaging

As with any other bodily activity, all brain activity, from cell organelles to synapses, to neurons, and networks requires adenosine triphosphate (ATP) [39]. Because neurons generate most of their ATP through oxidative metabolism, they rely heavily on a continuous supply of oxygen to fuel mitochondrial ATP production. As a result, when any cognitive activity takes place, from simple movements to solving mathematical equations, the area of the brain responsible for this activity has a local higher energetic requirement, causing a greater uptake of oxygen in the area [40]. As oxygen is taken up by the tissue in the area, signals are sent to the body to dilate the vessels around the tissue, resulting in higher blood flow compared to baseline to compensate for the used oxygen in the area. The body, however, overcompensates the amount of oxygen needed in what is called the hemodynamic response [41] elaborated on in Section 2.2.3.

2.2.3. Blood Oxygen Level Dependent Signal

To observe neural activations, fMRI scans utilize the Blood Oxygen Level Dependent signal, BOLD for short. This effect was first observed in 1990 by Ogawa and colleagues in the rat brain [42] and subsequently explored in the human brain by three separate research teams [43, 44, 45]. When neuronal activation occurs, the local energy demand drives an overcompensation of oxygen requirement in the area. Due to the overcompensation of oxygen delivery to the tissue, there is more oxyhemoglobin present in the tissue compared to when there is no activation in the area. Hemoglobin is the molecule in the body responsible for the delivery of oxygen to tissues and contains the compound heme. Heme has a central iron atom, and as iron is a ferromagnetic element, it causes distortions in a magnetic field [46]. However, when hemoglobin is in it's oxygenated form, the oxygen it transports shields the iron, causing a decrease in its ferromagnetic properties. This in turn causes the activated tissue, with a higher concentration of oxyhemoglobin, to produce a higher signal in the MR scanner. Across multiple images across time the difference in signal in specific voxels between consecutive images allows to highlight the areas of the brain with neuronal activation. This phenomenon is known as the hemodynamic response and is shown in Figure 2.3.

2.2.4. Approaches

The two most prominent ways of assessing brain activity using magnetic resonance are task-based fMRI and resting-state fMRI. Task-based fMRI relies on a temporally defined

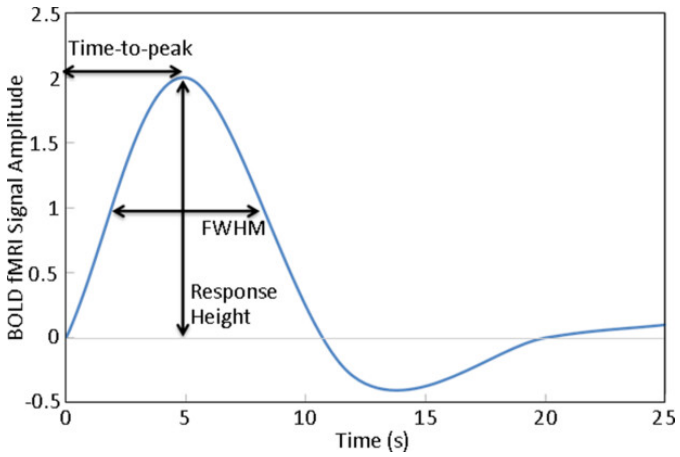

Figure 2.3.: Graph showing a standard hemodynamic response function (HRF). The graph shows time to peak (5s), the full width at half max (FWHM), and the response height of BOLD signal over time. The original figure from [47] with permission from John Wiley and Sons.

stimulus during which we expect to see differences in brain activations compared to baseline. Resting-state fMRI, on the other hand, attempts to observe co-activations that happen in the brain while it is doing nothing in particular. Both of these approaches tell us distinct information about the happenings in the brain and require different analytical methods.

Task-Based

In task-based fMRI, participants perform a specific cognitive, sensory, or motor task while brain activity is recorded, allowing researchers to identify regions involved in particular functions. This approach is based on assessing BOLD timecourses for similarity with the task timecourse, revealing areas where neural activity matches with task demands.

A classic example of a task-based fMRI paradigm is the finger-tapping task. In this paradigm, participants are instructed to repeatedly tap their fingers in response to a visual or auditory cue, alternating between periods of tapping and no movement. The resulting contrast in BOLD signal typically shows increased activation in the primary motor cortex, supplementary motor area, and cerebellum, corresponding to the motor control network [48]. This simple yet robust design makes the finger-tapping task a standard tool for validating fMRI setups and studying motor function. Within this thesis, a task-based fMRI approach was employed. While the participant does not do any specific task during scanning, the stimulation itself provides the contrast. The stimulation can be seen as an event or a task for which the contrast is computed.

Task-based fMRI studies provide critical insights into the functional organization of the brain by mapping specific processes to distinct cortical and subcortical regions. They allow researchers to test hypotheses about which brain areas are responsible for specific

behaviors or cognitive phenomena.

Resting State

In resting-state fMRI, brain activity is measured while participants are not engaged in any specific task, typically lying still with eyes open or closed. This approach captures spontaneous fluctuations in the BOLD signal over time, which are thought to reflect the brain's baseline functional organization [49]. Rather than relying on externally timed stimuli, resting-state fMRI examines temporal correlations between BOLD signals in different brain regions to identify networks that co-activate at rest. For example, regions within the so-called default mode network show strong functional connectivity when the brain is at rest [50]. The ability to track interconnected networks across individuals has made resting-state fMRI a valuable tool for studying large-scale brain organization. In this thesis, resting state fMRI scans are utilized for targeting outlined in Section 3.4.4. Due to the limitation of TMS to only stimulate cortical areas, functional connectivity patterns are utilized to target deep brain regions through their co-activation with cortical regions; in our specific case, the inverse relationship of firing between the sgACC and the dlPFC, the relationship between which can be effectively modulated using TMS [34]. Resting-state fMRI studies reveal how the brain maintains functional connectivity in the absence of explicit tasks, offering insights into its functional architecture. They allow researchers to investigate how brain networks differ across individuals, states, or clinical conditions. Resting-state approaches are also often combined with and complement task-based studies by providing a broader picture of the brain's communication patterns.

2.3. Concurrent TMS-fMRI

Concurrent transcranial magnetic stimulation and functional magnetic resonance imaging (TMS-fMRI) combines causal brain stimulation with whole-brain imaging. This integration provides a powerful means to investigate both the direct physiological consequences of TMS and its influence on distributed brain activity during cognitive processing. However, performing TMS inside an MRI scanner presents substantial technical and methodological challenges, including precise temporal coordination of stimulation, magnetic field interference, and accurate spatial targeting of the stimulated site. The following sections outline how these challenges are addressed through stimulation interleaving and neuronavigation, and demonstrate the range of applications that make concurrent TMS-fMRI an indispensable tool for probing human brain function.

2.3.1. Stimulation Interleaving

A major challenge when conducting concurrent TMS-fMRI experiments is the timing of stimulation. Since both TMS and fMRI are reliant on magnetic principles they can cause each other to interfere as can be seen in Figure 2.4. Due to this, proper interleaving of the stimulation is required in order not to corrupt the data, as an improperly timed stimulation can result in signal dropout in the acquired image or corrupted data.

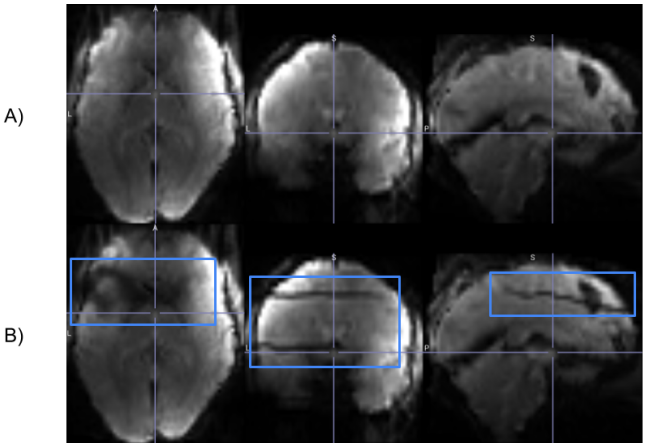

Figure 2.4.: Saggital, axial, and coronal images of volumes of a TMS-induced artefact (B) scan compared to a non-corrupted volume (A) during an EPI stimulation run. The darker parts of volume (B) show signal dropout in the acquired volume.

In our experiments, we rely on EPI sequences, which are particularly sensitive to magnetic disturbances during gradient switching and signal readout. To avoid introducing artifacts, we therefore synchronize the delivery of TMS pulses with the timing of the EPI sequence. Specifically, stimulation is applied in the short gaps between volume acquisitions, ensuring that no pulse coincides with the critical periods of signal detection [51] as can be seen in Figure 2.5.

This interleaving strategy requires precise calibration, as even a slight mistiming can lead to widespread signal dropout across the brain. In practice, this means that the temporal pattern of stimulation is constrained by the repetition time of the sequence, limiting the range of stimulation protocols that can be applied. While this synchronization allows us to combine the causal intervention of TMS with the spatial coverage of fMRI, it also highlights the technical compromises inherent in concurrent TMS-fMRI research.

2.3.2. Neuronavigation

Largely used in surgical applications, neuronavigation [52] has proven to be of tremendous utility in the use case of concurrent TMS and fMRI. The technology is reliant on the use of infrared (IR) cameras, reflective material, and triangulation. Our setup consists of the infrared camera, two trackers (one for the subject and one for the coil), and a tracked pointer. The trackers consist of a well-defined body and three reflective spheres. The camera constantly sends out an infrared light, which is then reflected off the three spheres of the trackers back into the sensors on the camera.

If the distances between the three infrared spheres can be measured, and the exact dimensions of the tracker are known, then both the exact tilt, rotation, and position of the tracker can be calculated using triangulation [53]. This is because, as the object itself rotates, the perceived distances between the tracker sphere change from the perspective

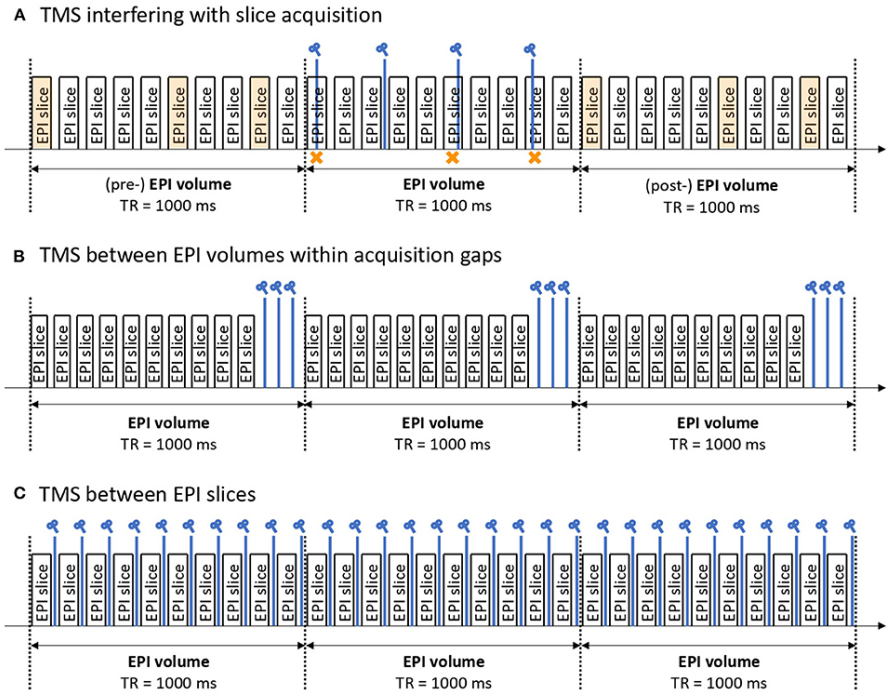

Figure 2.5.: Example of concurrent TMS-fMRI protocols. There are three possible ways to apply TMS pulses during fMRI simultaneously. (A) A method enabling TMS to interfere with EPI slices. Perturbed EPI slices (indicated by an orange cross) are sacrificed and replaced by slice interpolation, typically from the volumes before and after the volume of interest (indicated by orange EPI slices). (B) A method to insert a gap time between EPI slices and apply TMS pulses meanwhile. (C) A method to interleave TMS pulses with EPI slices. Figure and shortened caption acquired from [51], published in Frontiers in Psychiatry under the Creative Commons Attribution (CC BY) license.

of the camera. These changes in distances allow us to calculate the distance of the tracker and its rotation.

Mounting of the subject tracker is a bigger issue than the mounting of the coil tracker. While the coil tracker can be fixed to the coil using simple tape, the subject tracker needs to be attached to the subject via tissue. This increases complexity as the subject's body needs to be registered to the generated model in the neuronavigation software [54]. Outside of the scanner, the tracker is generally mounted onto the subject by taping the tracker to the subject's forehead using skin-safe tape. This approach comes with its own precision challenges, in particular, the subject inducing registration errors by movement of their forehead skin. This is generally mitigated during TMS by attaching the tracker to the opposite side of the head compared to stimulation, as stimulation itself can cause eyebrow twitches on the same side through nerve stimulation, decreasing the impact of motion on accuracy. While it has its downsides, this method is generally considered good

Figure 2.6.: An image of our neuronavigation setup and MR scanner.

enough for live neuronavigation with TMS outside of the scanner. Inside the MR scanner, however, the subject is lying inside the bore, meaning that a neuronavigation tracker would not be visible to the neuronavigation camera. For this, we use a maxilla tracker mount.

The maxilla, or the upper jawbone, is a part of the skull that houses the brain. This means that the maxilla is always in the same position relative to the brain. To fix the subject tracker, we utilize a maxilla tracker mount, a 3D-printed piece of plastic that is placed in the subject's mouth and extends a couple of centimeters above their head. The upper teeth are fixed to the maxilla, so the mouthpiece is attached to the subject's upper teeth through the use of dental putty for getting tooth molds. The tracker is then attached to the extension of the mount and can be used for neuronavigation [55].

This technology allows us to have the exact site of stimulation during concurrent TMS-fMRI scanning and stimulation sessions. Not only is this convenient for targeting, when precise targeting is necessary, it also allows researchers to go back and check the electric field generated in the subject's brain as a result of the stimulation using E-field simulation software like SimNIBS.

2.3.3. Applications

Early studies combining TMS and fMRI were mostly performed sequentially, meaning that TMS is applied outside the scanner before or after fMRI, to monitor lasting changes. Through interleaving strategies, researchers have been able to overcome technological challenges and allow for stimulation inside the MR scanner. This concurrent application of TMS and fMRI allows to reveal the immediate effects of TMS on the brain and its cortical and subcortical networks. Using this combination of methods researchers gained

a valuable tool for not only researching the neural consequences of stimulation, but also to causally investigate the pathways of the human brain. These aspects give us a clearer view of how the technology works, what it can show us, and how it can be made better. These are all important considerations for how we can have more personalized treatments and come closer to an understanding of how the brain works and how it contributes to cognition. In this section, the research implications of concurrent TMS-fMRI are discussed, and how they can contribute to the clinical and cognitive science knowledge bases.

Investigating the effects of TMS on the brain

Most importantly for cognitive science, concurrent TMS-fMRI allows researchers to investigate the pathways of the human brain causally. The concurrent use of the two technologies not only allows the observation of signal propagation right after stimulation, but also allows for the combination of stimulation with cognitive tasks, observing the interaction between stimulation and said tasks. This is a highly valuable tool, combined with the fact that TMS allows both for excitation and inhibition; the combined use allows us to explore previously inaccessible aspects of human cognition. This section looks at the uses of concurrent TMS-fMRI in fundamental science, probing the human brain, in vivo, without major bodily alterations.

Mapping Brain Networks Using TMS The first ever application of TMS-fMRI showed how concurrent TMS-fMRI can be used to causally investigate brain pathways and came from Bestmann and colleagues, who explored how stimulation of a single cortical region propagates through functionally connected networks. In their study, TMS was applied over the dorsal premotor cortex (PMd) while fMRI simultaneously measured BOLD responses throughout the brain. The results revealed not only local activation under the stimulation site but also significant modulation in remote but functionally connected regions, such as the supplementary motor area, primary motor cortex, and parietal regions [56]. These findings demonstrated that the impact of TMS extends beyond the targeted cortical area, influencing the dynamics of entire functional networks in a manner consistent with known anatomical and functional connectivity. By directly visualizing the spread of stimulation-evoked activity, this study provided causal evidence for the existence of distributed motor networks. It showed how concurrent TMS-fMRI can be used to map directional connectivity between cortical regions in the living human brain.

TMS Induced Cognitive Enhancement TMS has a unique power to enhance cognitive ability through the stimulation of specific areas. TMS studies have shown, for example, that stimulation in the language areas, causing pre-activation in the regions implicated in speech comprehension, increases the subjects' performance on language tasks, causally implicating the regions significance in language processing [57]. Studies like this, however, do not provide the full picture as they do not show how brain networks can reorganize at the time of stimulation. Therefore, fMRI comes in to give us a deeper understanding

of how the regions of stimulation might enhance or decrease performance on a given cognitive task. Recent concurrent TMS-fMRI work has demonstrated the unique strength of this approach for uncovering such mechanisms. For instance, Hermiller and colleagues applied theta-burst TMS, a patterned stimulation protocol designed to emulate the brain's natural theta-frequency rhythms linked to learning and memory [58], during fMRI to a cortical node functionally connected to the hippocampus while participants encoded visual scenes. They found that stimulation immediately increased hippocampal activity and improved subsequent memory performance, while control stimulation conditions produced no such effects. These findings provide direct causal evidence that network-targeted stimulation can modulate deep-brain regions in real time, linking stimulation-induced neural activity to cognitive enhancement within the same experimental window [28]. These results highlight how concurrent TMS-fMRI can reveal the causal dynamics between brain networks and cognition, demonstrating that precisely timed, rhythm-specific stimulation can directly modulate deep memory-related structures and thereby enhance cognitive function.

TMS-EEG-fMRI The use of TMS-fMRI can be further enhanced with EEG. One of the biggest recent breakthroughs in this field of brain scanning and stimulation has been the development of technology for monitoring brain waves using EEG concurrently with the TMS-fMRI. This triad of TMS-EEG-fMRI allows researchers to not only monitor the cortical and subcortical activity, but also the brain states at the time of stimulation. EEG or electroencephalography is a method for capturing the waves of brain activity. These waves correspond to brain activity under the generally 64 electrodes of an EEG cap. The frequencies captured by an EEG are split into 5 categories: delta, theta, alpha, beta, and gamma, representing an increasing frequency coupled with an increasing alertness [59]. This imaging method has a very high temporal resolution, meaning it can capture sub-second brain activity, but a very low spatial resolution as it can only capture cortical activity limited to the positions under the electrodes, which are located around the head. The combination of EEG and fMRI is a logical one as fMRI, on the other hand, has a very high spatial resolution, being able to capture generally 1mm by 1mm by 1mm area of both the cortex and subcortical areas, but does not have a very high temporal resolution, meaning it can generally only capture activity on the order of magnitude of seconds. Peters and colleagues revolutionized concurrent imaging and stimulation methods by combining concurrent TMS-fMRI with EEG, allowing for both high temporal resolution and spatial resolution of brain activity. In doing so they also found that brain states have a modulatory effect on the ability of TMS to excite the brain. More specifically, the researchers found that when the brain has a higher prevalence of alpha power, or frequencies that correspond to an awake but restful state, the BOLD signal as a result of TMS is inhibited [60]. This finding shows that the brain states at the time of stimulation have an effect on how well the brain can be stimulated, or how prone it is to activation. If you are in a restful state, then the stimuli you perceive cause less activation, inherently showing less processing of the stimulus. Studies such as this provide a better picture into how the different aspects of brain activity work together to produce cognition and, for

example, why being in a more restful state might make things harder to process, compared to more alert states such as Beta waves, where the researchers found no inhibitory effect [60].

Investigating TMS itself

Most relevant for its clinical implications, the ability to observe the effects of TMS during an fMRI scan allows researchers to analyze the neural consequences of the technology. TMS and its use for treatment are quite novel, and its optimization is pivotal in increasing its efficacy in both clinics and laboratories. Questions such as what frequency of stimulation induces most brain activity, what stimulation targets are most efficacious for activating specific brain networks, and at what time can stimulation be used to activate the brain most effectively. These are all questions which concurrent TMS-fMRI can help researchers answer, allowing for better treatment methods and more accurate scientific practices.

Stimulation Intensity Impacts Concurrent TMS-fMRI has proven invaluable for elucidating the causal propagation of stimulation effects across cortical and subcortical networks, as shown by Tik and colleagues. They used concurrent interleaved TMS-fMRI to map the acute network-level consequences of dlPFC stimulation, showing that single pulses over the dlPFC evoke BOLD activation patterns that closely mirror a well-characterized resting-state network encompassing the anterior cingulate cortex, insula, thalamus, and widespread cortical regions [61]. In a later study, the authors systematically varied the stimulation intensity over the left dlPFC while recording whole-brain BOLD responses to characterize individual dose-response profiles. Using a high-sensitivity concurrent TMS-fMRI setup, they found that stimulation at 100% of the active motor threshold elicited the strongest group-level activation, engaging a network spanning bilateral dlPFC, premotor and supplementary motor areas, anterior and posterior cingulate cortices, insula, thalamus, and basal ganglia. Crucially, individual analyses revealed substantial variability in excitability patterns, with some participants showing maximal responses at subthreshold intensities and others exhibiting nonlinear response curves, indicating that stimulation intensity does not linearly translate into cortical activation. These findings demonstrate that the neural effects of TMS are shaped by complex, region-specific dynamics rather than by simple proportional scaling of stimulation dose. By directly mapping the neural consequences of different stimulation intensities, [62] provided causal evidence that the dlPFC's excitability and its connected network responses vary substantially between individuals, underscoring the need for personalized calibration of stimulation parameters to optimize both mechanistic and therapeutic outcomes.

Brain State Impacts Although the temporal resolution of fMRI itself is limited, precise application of TMS at specific timepoints allows to assess effects of state dependency. Grosshagauer and colleagues demonstrated how this methodology can be leveraged to investigate the influence of brain state on TMS effects both locally and across large-scale networks. In their study, individualized targets in the left dlPFC were defined based on

functional connectivity with the sgACC, a region strongly implicated in depression and treatment response. Using chronometric interleaved TMS-fMRI, the authors delivered 10 Hz triplets of TMS during both rest and task performance, showing that the precise timing of stimulation relative to cognitive processing produces distinct BOLD responses in the sgACC and dlPFC. Importantly, stimulation administered during optimal task-related brain states yielded more consistent and pronounced modulation of the sgACC compared to stimulation during rest, suggesting that the underlying brain state critically shapes the neural impact of TMS. These findings highlight the importance of considering cognitive and temporal context in stimulation design and underscore the potential of state-informed TMS protocols for improving both mechanistic understanding and therapeutic outcomes [63]. This demonstrates that TMS is not merely a tool for probing isolated brain regions, but a dynamic method capable of interacting with ongoing neural processes to modulate distributed networks in a temporally precise and functionally meaningful way.

Connectivity Impacts Concurrent TMS-fMRI has also been used to explore how stimulation modulates large-scale functional networks in the human brain, offering causal insight into how neuroplastic changes unfold across systems. Ge and colleagues applied repetitive TMS at 1 Hz to the right dlPFC during fMRI acquisition in patients with treatment-resistant depression to assess how acute changes in functional connectivity relate to later therapeutic outcomes. Their results showed that during rTMS, widespread but transient alterations in connectivity between prefrontal, parietal, insular, and thalamic regions, and that these acute changes predicted approximately 30% of the variance in clinical improvement following a four-week course of rTMS treatment. This work demonstrated that TMS does not act locally, but rather triggers distributed, state-dependent network reconfigurations that reflect the brain's neuroplastic potential [64]. In doing so, it provided causal evidence that large-scale connectivity changes induced by TMS may serve as mechanistic markers of treatment response and highlighted the capacity of concurrent TMS-fMRI to link acute network-level dynamics with longer-term behavioral and clinical outcomes.

2.4. Cognitive Theories

Since its formal conception, cognitive science has evolved through several paradigms. From cognitivism, to embodied and 4E approaches, and more recently, predictive processing, among many others. Each framework offers a distinct view on what cognition is, where it happens, and how the brain contributes to it. These theoretical differences are not merely philosophical; they fundamentally shape how we design experiments, interpret neural data, and understand the relationship between brain activity and cognition. TMS–fMRI, as a method that both perturbs and measures neural activity, can be positioned differently within the theoretical lenses of cognitivism, 4E cognition, and predictive processing. Understanding these theoretical positions is therefore essential for interpreting what TMS–fMRI studies actually reveal about the nature of cognition itself.

2.4.1. Cognitivism

Within the cognitivist tradition, the mind is conceptualized as a symbol-manipulating information-processing system, where cognition consists of formal operations on internal representations according to syntactic rules, and the brain functions as the physical hardware that implements these abstract computational processes [65, 66, 67]. This framework aligns naturally with the logic of TMS–fMRI research, as both assume that cognitive processes can be localized to specific functional architectures or computations within the brain. TMS, in this view, offers a means to test the causal necessity of specific regions in executing particular cognitive computations. Disrupting a node in the information-processing chain should produce measurable effects on task performance. Meanwhile, fMRI measures the representational structure of cognitive processes. Within the cognitivist framework, TMS–fMRI provides a causal method for linking representational computations to neural substrates. By perturbing a region implicated in a specific mental operation and observing corresponding BOLD and behavioral changes, researchers can test whether that region is necessary for the computation in question. This approach treats the brain as a modular system of specialized processors, each implementing distinct aspects of the cognition.

2.4.2. 4E Cognition

In contrast to cognitivism's emphasis on internal representations, embodied and 4E cognition argues that cognition is not confined to the brain but arises through interaction with the body, environment, and context [1]. The 4E approach encompasses four interrelated principles: embodied cognition, which emphasizes that cognitive processes depend fundamentally on bodily states and action systems; embedded cognition, which situates the mind within environmental contexts; enactive cognition, which views the mind as emerging through active engagement with the world; and extended cognition, which proposes that tools and environmental structures can become functional components of the mind. At first glance, TMS–fMRI may appear incompatible with these frameworks, given its focus on brain activity. However, this method can be reframed as a tool for studying brain–body–environment coupling rather than purely intracranial computation. For instance, state dependence is a prominent concept in neuroscience which has shown that in different contexts the brain responds differently to the same stimuli. The context in which the brain and body are embedded alters how stimulation affects them, as demonstrated by a growing body of work on state-dependent effects of TMS [68]. From a 4E perspective, concurrent TMS–fMRI can explore how neural perturbations alter embodied and context-dependent patterns of engagement. Such an approach redefines the unit of analysis from isolated cortical modules to dynamically coupled brain–body–environment systems.

2.4.3. Predictive Processing

Predictive processing conceptualizes the brain not as a passive recipient of sensory data but as an experience-driven prediction machine that uses prior expectations, past experiences, and top-down hypotheses to actively interpret incoming signals [69, 70]. In this view, perception, action, and learning arise from the brain's effort to minimize prediction error by continuously updating its generative models. Higher cortical areas generate expectations about lower-level activity, while mismatches between predictions and sensory evidence propagate upward to revise those expectations. Predictive processing is particularly well-suited to investigation via TMS–fMRI as the method allows for direct causal testing of predictive hierarchies. By perturbing regions involved in generating predictions or processing prediction errors, researchers can observe how disruption propagates through networks and affects both BOLD responses. For example, TMS can be used to arrest function at specific nodes in the cortical hierarchy, while fMRI captures the downstream consequences across distributed networks [22] as exemplified in Section 2.1.3. Predictive processing offers a unifying framework for interpreting TMS–fMRI results: by perturbing regions involved in predictive hierarchies and measuring changes in BOLD and connectivity, researchers can test hypotheses about the direction of top–down and bottom–up message passing. This approach connects to computational modeling and generative frameworks, enabling researchers to formalize predictions about how specific perturbations should alter precision weighting, belief updating, or the balance between prior and evidence, making it a great theoretical lens for concurrent TMS–fMRI studies as a causal probe of the brain.

2.4.4. Implications

Beyond serving as a methodological tool within existing theoretical frameworks, TMS–fMRI and this study specifically makes a distinctive contribution to cognitive science by challenging assumptions about the stability and organization of the neural substrate underlying cognition. Cognitive theories frequently assume a relatively fixed functional brain mappings, treating specific regions or networks as consistently implementing specific cognitive operations. However, the brain is highly dynamic, characterized by fluctuating excitability [71, 72]. TMS–fMRI offers a causal method to test if the assumed mappings hold across time and to examine how cognition emerges and stabilizes within such a variable system.

By applying perturbations across different time points, we can assess the consistency of causal effects and determine whether stability is a true property of the system or an emergent feature arising from underlying dynamic networks. This approach encourages cognitive science to reconceptualize cognition not as computation within static modules, but as a process of continual reorganization and adaptive coordination. The combination of TMS with fMRI is particularly powerful for mapping this dynamic organization, as it exposes how functional architectures reconfigure across states.

Moreover, while TMS may appear "unnatural" compared to sensory or cognitive tasks, both artificial and natural stimuli activate the same underlying neural architecture [73]. The difference lies in the form of input, not in neural principles. Synthetic stimulation allows precise and controlled causal testing of the same mechanisms that natural stimuli

continuously engage, and differences between synthetic and natural effects are likely quantitative rather than qualitative, differing in the isolation of input from confounding states. This positions TMS–fMRI as a complementary tool for cognitive science, comparing controlled neural perturbations to naturally occurring cognitive processes and providing a direct empirical route to study how dynamic brain activity gives rise to consistent cognitive functions. Ultimately, TMS–fMRI encourages a conceptual shift from static, representational views of cognition towards dynamical and process-based frameworks that account for variability, adaptability, and context sensitivity, reframing cognition itself as emergent stability within a continuously fluctuating brain.

3. Methods

The following chapter outlines the specific methods that were utilized in the acquisition of data for this study. It covers hardware and software used, subject demographics, experimental setup, and analysis with all associated information.

3.1. Hardware

3.1.1. fMRI

During all MRI scans, we used a Siemens Prisma Fit 3T scanner for image acquisition (Siemens Healthineers, Erlangen, Germany). During the intake session we acquired a high-resolution anatomical scan using a Siemens Head/Neck 64 channel RF coil. During the stimulation sessions, we used three 7-channel surface receive coils [74] for image acquisition; one coil was mounted underneath the TMS coil on the scalp, the second coil was positioned on the contralateral side of the head and the third coil was placed in occipital position.

3.1.2. TMS

For stimulation, we used the MagVenture MRi-B91 figure-of-eight stimulation coil in combination with the MagPro X100 stimulator (MagVenture, Farum, Denmark). During the intake session, the stimulation coil was used in isolation, and during the fMRI stimulation sessions, a 7-channel surface receive coil [74] was directly attached underneath the TMS coil.

3.1.3. Neuronavigation

For the live neuronavigation during the intake session and stimulation session we used the Polaris Vega VT (Northern Digital Inc., Waterloo, Canada) infrared camera. During the intake session, we used a subject tracker taped to the subject's forehead and a tracker with a different tracker geometry attached to the TMS coil. For coil positioning before stimulation, we used the BrainSight (Rogue Research Inc, Montreal, Canada) software in the coil-centric view. During the stimulation, we used an in-house developed live tracking software for saving the positions continuously.

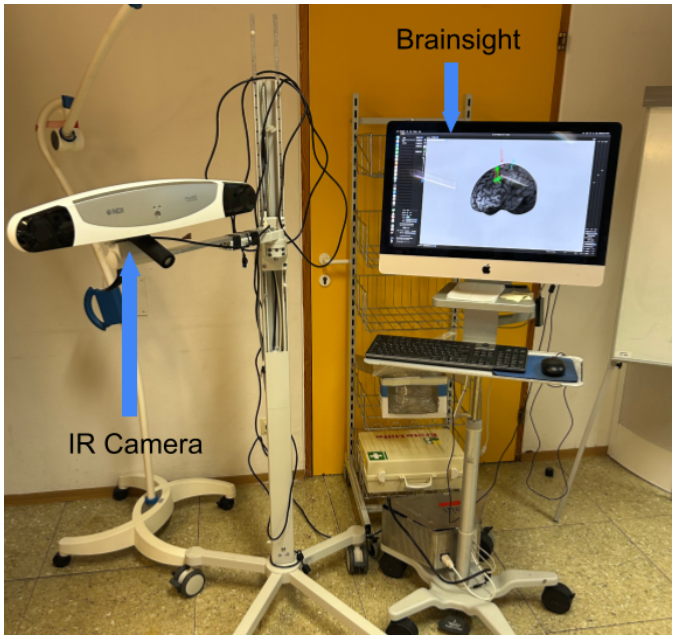

Figure 3.1.: Neuronavigation setup used for targeting. Shown are the Polaris Vega VT infra-red camera (left) and a computer with the BrainSight software with a dlPFC target (right).

3.2. Subjects

3.2.1. Subject Recruitment

Subjects were recruited using university communication channels. They were informed about the procedure of the experiment as well as any possible contraindications. To ensure participant safety, a meticulous screening procedure for possible contraindications to either TMS or fMRI was performed. Furthermore, we aimed for equal gender balance in our sample. All in-vivo studies performed within this thesis were in agreement with the Declaration of Helsinki and as part of a larger study approved by the institutional review board. Participants were required to give their written informed consent, which they could withdraw at any point in time without stating a reason. The participants were also refunded financially with 10 Euros per hour.

3.2.2. Subject Demographics

Participants for this study were healthy young adults. All of them were from central Europe and resided in the Vienna region. The subset of subject data selected for the results section of this thesis was based on the quality of data. Ten datasets were collected, but sub-rel001 dropped out after the first stimulation session and sub-rel005's ses-02 singlets data was corrupted by TMS artefacts giving us eight full datasets.

Participant	Age	Gender	ses-01	ses-02	ses-03
sub-rel001	26	Male	2 May	9 May	-
sub-rel002	18	Male	6 May	16 May	23 May
sub-rel003	25	Male	7 May	21 May	23 May
sub-rel004	25	Female	23 May	4 June	6 June
sub-rel005	25	Female	8 July	23 July	25 July
sub-rel006	28	Male	30 July	10 September	17 September
sub-rel007	22	Female	17 September	26 September	3 October
sub-rel008	19	Female	24 September	30 September	7 October
sub-rel009	28	Male	24 September	24 October	12 November
sub-rel010	32	Female	24 September	24 October	5 November

Table 3.1.: Age, gender, and session dates for participants sub-rel001 to sub-rel010

3.2.3. Screening Procedures

Participants were asked to fill out a safety questionnaire for both MRI and TMS compatibility (see Appendix). For a more thorough explanation of the safety considerations for TMS see the Section Safety in the TMS chapter in Background information and the TMS subject form in the Appendix. Only if no contraindication was indicated by the participant, the respective person was eligible for the study. All screening procedures were performed at the beginning of ses-01.

3.3. Experimental Pipeline

The experimental pipeline follows a strict order, which was outlined in detail in the following section. A simplified version of the pipeline is shown in Figure 3.2 below.

3.3.1. Intake Session

The first session, titled ses-01, was an intake session required for setting up the stimulation sessions (ses-02 and ses-03). During the intake session, the following steps were taken in the respective order.

The session started with a briefing of the participant on the experimental procedure. This included an explanation of the principles of magnetic resonance and transcranial magnetic stimulation, as well as their safety requirements. The experimental steps of the first session were then explained. The subject then signed informed consent forms for TMS and fMRI studies shown in the Appendix and was made MR compatible by removing any jewelry and piercings and changing into scrubs.

The subject was positioned in the MR scanner, where a 5-minute T1-weighted anatomical scan was be conducted, followed by a 10-minute resting state scan where the subject was instructed to lie as still as possible, not think about anything in particular, and to

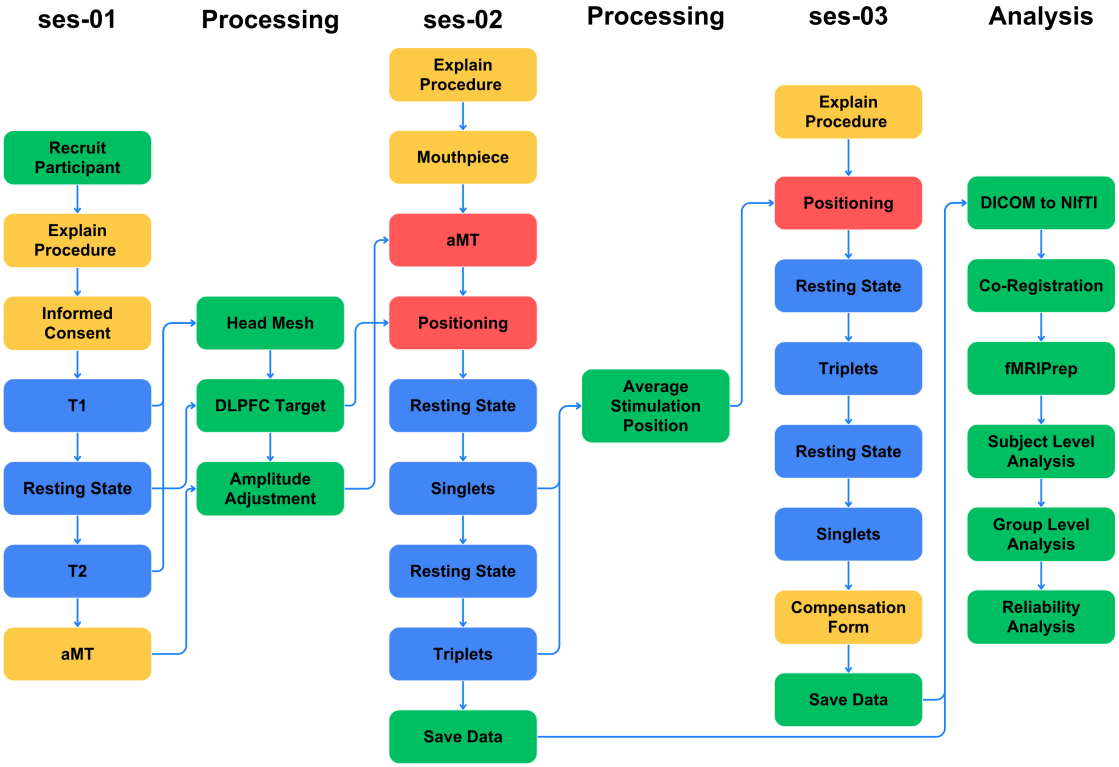

Figure 3.2.: Flowchart of the complete experimental pipeline. Green bubbles represent steps taken outside of the experimental trial. Yellow bubbles represent steps taken outside of the scanner room. Red bubbles represent steps taken inside the scanner room but outside of the MR scanner itself. Blue bubbles represent steps taken inside of the MR scanner.

try not to fall asleep as it could cause movement that would corrupt the data. Finally, a 5-minute T2-weighted anatomical scan was be conducted.

After the scans were finished, the subject was taken out of the scanner room, allowed to change, and briefed on the active motor thresholding procedure. First, the setup was shown to the subject, and they are instructed to sit down and given hearing protection.

The experimenter put the coil to the subject's head, then counted down from 3 to 1, and gave the subject an example pulse at 60% maximum stimulator output (MSO). After confirming that the subject is okay with the discomfort of stimulation, the thresholding session was performed as outlined in Section 3.4.1.

3.3.2. Inter-Session Processing

Between the intake session and the first stimulation session, the data acquired was processed to obtain the stimulation target and the adjusted dose. Firstly, the charm command was run using SimNIBS [10] using the T1 and T2 weighted anatomical scans of

the subject to generate a tissue-segmented model of the subject's brain. Subsequently, the stimulation target was generated based on the functional connectivity scan, the procedure for which is outlined in Section 3.4.4. Based on this target and the SimNIBS model, an optimal coil position, including coil center, rotation and tilt, was calculated using SimNIBS [75]. This target was then loaded into BrainSight to check for validity, as some targets are not reachable by the coil and cannot be used for online stimulation. The target was then used in an in-house developed software to get the adjustment scaling factor. This procedure is outlined in Section 3.4.5. With the target and the adjustment scaling factor, the stimulation sessions may proceed.

3.3.3. Stimulation Sessions

The stimulation sessions, labeled ses-02 and ses-03, were temporally dependent on each other. The first stimulation session should have take place at least one day after the intake session to allow sufficient time to process the data from the intake session. Similarly, the time between ses-02 and ses-03 was required to be at least 48h to provide ample time for the brain to return to its baseline state. Ideally, measurements were not separated by more than 10 days. Lastly, ses-02 and ses-03 needed to take place at the same time of day to account for daily fluctuations of functional connectivity, as they could have affected and confounded the data [71].

The subject was first welcomed to the laboratory, and a recapitulation with a more in-depth explanation of the procedure from ses-01 was given to them. The procedure explanation is stated in this section.

Afterwards, a mouthpiece was tailored to their top row of teeth. This was used to create a maxilla mount for the subject neuronavigation tracker [55]. A dental impression putty was attached to a 3D printed mouthpiece, and the subject was instructed to bite down on the putty so that the leg of the tracker sticks out centrally and to wait roughly 30 seconds until the putty hardens. They could then take the mouthpiece out, and it was prepared by taping the neuronavigation tracker to the mount.

The subject was then told to change into scrubs and remove any jewelry and metallic objects from their body. The rest of the session took place in the scanning room.

Afterward, an active motor thresholding session took place inside the scanner room. This was to account for the daily fluctuations in the active motor threshold [72]. The 5 millimeter width of the RF coil attached to the stimulator coil increased the coil-cortex distance, reducing the effects of TMS by roughly 2.8%MSO per milimeter [76]. This combined with other factors such as bore and cable length necessitated the remeasurement of the aMT with the TMS-fMRI setup. Therefore, the same procedure was conducted as is outlined in Section 3.4.1. The active motor threshold acquired was then scaled using the scaling factor based on the subject's individual anatomy. The procedure used to get this scaling factor is outlined in Section 3.4.5 and the scaling factors for each subject are shown in Table 3.2. The scaled stimulation intensity was then used throughout both ses-02 and ses-03.

Afterwards, the subject was asked to lie down on the scanner bed and place their mouthpiece on the maxilla to conduct subject registration procedures. Extra care was

Figure 3.3.: Maxilla mouthpiece tracker mounts. Unused 3D printed maxilla mount (left), used maxilla mount with dentistry putty (center), and maxilla mouthpiece mount with neuronavigation tracker attached (right).

taken to make sure the registration error at the target site was less than 1mm. The procedure for registration is outlined in 3.4.2.

After registration, the subject was placed into the experimental setup, and coil positioning took place. Initially, the coil was placed onto the target region and held by the experimenter, and then fixed by another experimenter. Generally, the coil shifted in position and tilt when it was fixed in the mount, and therefore, the position was then adjusted by using the various axes of the coil holder. Great care was taken during the positioning to make sure the position was less than 2mm away from the target and less than 5° off in tilt and rotation. Rotation was the most important element of positioning due to the angle at which the magnetic field intercepts the gyrus on which the dlPFC lies [77, 78]. Once the desired position was achieved, the actual image acquisition started.

The scanning protocol took the same form in both ses-02 and ses-03, with the exception of the singlets stimulation block and triplets stimulation block having a reverse order for ses-03 (the triplets block goes first, followed by the singlets block in ses-03). This was to account for any order confounds and to make sure that the subject was not startled by the first stimulation too much, causing motion confounds in ses-02.

Initially, anatomical scans were performed to acquire the accurate head position of the subject on the day to enable slice positioning. Then the first resting state scan was conducted. The data acquired during this scan were not utilized during this thesis, and the first resting state served largely as a means for the participant to acclimate to the complex setup. Then the first stimulation run occured.

The stimulation sessions were set up in the format outlined in Section 3.5.2. In ses-02, in the first stimulation run, the stimulation type was singlets, and in ses-03, the stimulation type of the first stimulation run was triplets. The subject was informed before the stimulation started that the run will start shortly and that the first stimulation may be startling. They were told to try to maintain their position.

After the first stimulation run, another 10-minute resting state was conducted. The

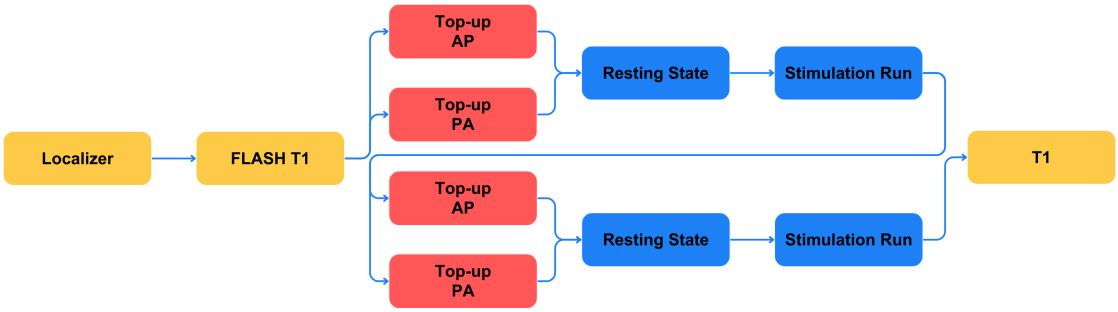

Figure 3.4.: Pipeline of the scans acquired during a stimulation session (ses-02 and ses-03). Yellow bubbles represent anatomical scans. Red bubbles represent adjustment scans used for co-registration. Blue bubbles represent functional scans.

functional connectivity data was not used for analysis for this thesis. The resting state scan was used mostly as a time for the subject to rest and for their brain to recover to baseline.

The next stimulation run followed the same format as the first, with the order of the stimulation protocols being reversed. This means that in ses-02, the stimulation type was triplets, and in ses-03, the stimulation type was singlets.

The last step of scanning was an MP2RAGE anatomical scan. This was again done as a fail-safe to be able to recover data. This concluded the session; the subject was told to change back into their clothes, after which they could leave.

Between ses-02 and ses-03, processing took place to acquire the average stimulation position for both triplets and singlets from ses-02. The average of the two average positions was then used for targeting during ses-03.

3.3.4. Pre-Processing

To pre-process the data, we use a standard fMRIprep pipeline. To improve the accuracy of co-registration achieved by fMRIprep, the echo-planar imaging (EPI) scans from each session are manually aligned to the T1 scan from ses-01 prior to running the further preprocessing using 3D Slicer [79].

3.3.5. fMRIPrep Boilerplate

The following paragraphs reproduces the official fMRIPrep citation and boilerplate text, which is required for all studies utilizing the fMRIPrep preprocessing pipeline to ensure proper attribution and methodological transparency.

Results included in this manuscript come from preprocessing performed using *fMRIPrep* 24.0.1 ([80]; [81]; RRID:SCR_016216), which is based on *Nipype* 1.8.6 ([82]; [83]; RRID:SCR_002502).

Preprocessing of B0 inhomogeneity mappings A total of 2 fieldmaps were found available within the input BIDS structure for this particular subject. A *B0*-nonuniformity

map (or *fieldmap*) was estimated based on two (or more) echo-planar imaging (EPI) references with `topup` ([84]; FSL None).

Anatomical data preprocessing A total of 1 T1-weighted (T1w) images were found within the input BIDS dataset. A preprocessed T1w image was provided as a precomputed input and used as T1w-reference throughout the workflow. A precomputed brain mask was provided as input and used throughout the workflow. Precomputed discrete tissue segmentations were provided as inputs. Precomputed tissue probabiilty maps were provided as inputs. Brain surfaces were reconstructed using `recon-all` [85], and the brain mask estimated previously was refined with a custom variation of the method to reconcile ANTs-derived and FreeSurfer-derived segmentations of the cortical gray-matter of Mindboggle [86]. A T2-weighted image was used to improve pial surface refinement.

Functional data preprocessing For each of the 9 BOLD runs found per subject (across all tasks and sessions), the following preprocessing was performed. First, a reference volume was generated, using a custom methodology of *fMRIPrep*, for use in head motion correction. Head-motion parameters with respect to the BOLD reference (transformation matrices, and six corresponding rotation and translation parameters) are estimated before any spatiotemporal filtering using `mcflirt` [87]. The estimated *fieldmap* was then aligned with rigid-registration to the target EPI (echo-planar imaging) reference run. The field coefficients were mapped on to the reference EPI using the transform. The BOLD reference was then co-registered to the T1w reference using `bbregister` (FreeSurfer) which implements boundary-based registration [88]. Co-registration was configured with six degrees of freedom. Several confounding time-series were calculated based on the *preprocessed BOLD*: framewise displacement (FD), DVARS and three region-wise global signals. FD was computed using two formulations following Power (absolute sum of relative motions, [89]) and Jenkinson (relative root mean square displacement between affines, [87]). FD and DVARS are calculated for each functional run, both using their implementations in *Nipype* [89]. The three global signals are extracted within the CSF, the WM, and the whole-brain masks. Additionally, a set of physiological regressors were extracted to allow for component-based noise correction [90]. Principal components are estimated after high-pass filtering the *preprocessed BOLD* time-series (using a discrete cosine filter with 128s cut-off) for the two *CompCor* variants: temporal (tCompCor) and anatomical (aCompCor). tCompCor components are then calculated from the top 2% variable voxels within the brain mask. For aCompCor, three probabilistic masks (CSF, WM and combined CSF+WM) are generated in anatomical space. The implementation differs from that of Behzadi et al. in that instead of eroding the masks by 2 pixels on BOLD space, a mask of pixels that likely contain a volume fraction of GM is subtracted from the aCompCor masks. This mask is obtained by dilating a GM mask extracted from the FreeSurfer's *aseg* segmentation, and it ensures components are not extracted from voxels containing a minimal fraction of GM. Finally, these masks are resampled into BOLD space and binarized

by thresholding at 0.99 (as in the original implementation). Components are also calculated separately within the WM and CSF masks. For each CompCor decomposition, the k components with the largest singular values are retained, such that the retained components' time series are sufficient to explain 50 percent of variance across the nuisance mask (CSF, WM, combined, or temporal). The remaining components are dropped from consideration. The head-motion estimates calculated in the correction step were also placed within the corresponding confounds file. The confound time series derived from head motion estimates and global signals were expanded with the inclusion of temporal derivatives and quadratic terms for each [91]. Frames that exceeded a threshold of 0.5 mm FD or 1.5 standardized DVARS were annotated as motion outliers. Additional nuisance timeseries are calculated by means of principal components analysis of the signal found within a thin band (*crown*) of voxels around the edge of the brain, as proposed by [92]. All resamplings can be performed with *a single interpolation step* by composing all the pertinent transformations (i.e. head-motion transform matrices, susceptibility distortion correction when available, and co-registrations to anatomical and output spaces). Gridded (volumetric) resamplings were performed using `nitransforms`, configured with cubic B-spline interpolation.

Many internal operations of *fMRIPrep* use *Nilearn* 0.10.4 [93], mostly within the functional processing workflow. For more details of the pipeline, see the section corresponding to workflows in *fMRIPrep*'s documentation.

Copyright Waiver

The above boilerplate text was automatically generated by fMRIPrep with the express intention that users should copy and paste this text into their manuscripts *unchanged*. It is released under the CC0 license.

3.3.6. Analysis

For analysis, we used standard General Linear Model analysis used for fMRI data. The analysis was conducted in Python using the Nilearn library [94] in combination with standard data analysis Python libraries such as Numpy and Pandas. The regressor we used was the stimulation timepoints convolved with HRF. To have cleaner data, we accounted for the following confounds derived from fMRIprep: *trans_x*, *trans_y*, *trans_z*, *rot_x*, *rot_y*, *rot_z*, *csf*, and *white_matter*. The three analyses conducted consisted of subject-level, group-level, and reliability analysis.

The subject-level analysis processed fMRI data for each subject, session, and protocol (singlets and triplets) independently using the Nilearn library for neuroimaging analysis. The pipeline begins by extracting stimulation onset times from H5 files containing experimental timing data, which are then convolved with the hemodynamic response function (HRF) to create the primary regressor. A first-level design matrix is constructed using Nilearn's *make_first_level_design_matrix* function, incorporated the stimulation

events along with eight motion and physiological confound regressors extracted from fMRIprep output files. The preprocessed BOLD data was smoothed with a 6mm FWHM Gaussian kernel and fitted to a General Linear Model using Nilearn's *FirstLevelModel*, with a binary brain mask resampled to match the functional data resolution. For each analysis, the General Linear Model(GLM) produced five statistical maps (z-scores, t-statistics, effect sizes, p-values, and effect variance), which were saved as NIfTI files along with visualizations showing activation patterns across multiple axial slices.

At the group level, we aggregated each subject's first-level contrast maps and run second-level GLMs with Nilearn's *SecondLevelModel*. The script first builds file paths from a configurable subject/session list, applies any exclusions, and loads the NIfTI images with NiBabel while validating all available data. It then constructs simple intercept-only design matrices in Pandas and fits separate second-level models for the singlets and triplets conditions, computing the group z-maps; results are visualized using Nilearn's plotting utilities. To directly compare conditions, the script stacks both sets of images, defines a two-column design: condition effect + intercept, computes the triplets vs. singlets contrast, and writes the resulting z-map.

Lastly, reliability was assessed as cross-session correlation of the parcel-wise effect size maps. The script loaded the Schaefer-2018 atlas with 400 parcels [95] and seven Yeo Networks [96], and built Nilearn's *NiftiLabelsMasker* to extract regional values from each NIfTI map, then organized these vectors into a Pandas DataFrame. It computed similarity between vectors with Pearson correlation, yielding within-subject cross-session correlations for each protocol and between-subject correlations for all subject pairs. Paired t-tests compared singlet vs. triplet cross-session consistency and self-similarity vs. between-subject similarity. Results are collated into a summary table and visualized with Seaborn.

3.4. Further Details on Preparations

3.4.1. Active Motor Threshold Acquisition

The stimulation intensity we utilized for the experiment was based on the subjects' active motor threshold. The procedure for acquiring the threshold was based on the procedure proposed by Schutter and van Hoink [97]. The subject was instructed to do an exercise with their fingers to attain pre-activation in the primary motor cortex before stimulation. This was done to lower the activation threshold by already having activation in the area before stimulation [98]. The exercise consisted of a squeeze of the index finger against the thumb on their right hand at maximum force for a second, followed by a squeeze of 50% of the maximum force, followed by a squeeze of 10% of the maximum force, which the subject was asked to maintain throughout the stimulation; this was equivalent to a slight contact between the index finger and the thumb which should not be strenuous.

The experimenter approximated the location of the primary motor cortex after which the subject was stimulated at 60% MSO in a grid-like pattern around the target with varying rotations of the coil in 2-second intervals until the maximum finger twitch response

was elicited. The researcher then maintained this position and rotation, and continued stimulation, decreasing the % MSO in 1-2% steps until the lowest possible amplitude at which half of the stimulations elicit a finger twitch response was found. This percentage was then noted and established as the subject's active motor threshold.

3.4.2. Subject Registration

During subject registration the actual head of the subject was mapped onto the digital model created by the BrainSight software using the aforementioned pointer. An initial landmark-based registration was conducted by touching the tip of the pointer to the subject's left tragus, nasion, and right tragus. These points were selected on the digital model based on the salience, protrusion, and visibility of anatomical landmarks on the head and the digital model. The left and right tragus and nasion are generally the most reproducible anatomical landmarks for registration. To further improve the registration accurate, additional samples were placed around the scalp, oriented in a cross-shaped pattern going from the left ear to the right and the forehead to the vertex of the head in roughly 2-centimeter increments. Lastly, an array of n by n points (depending on the subject's head size) was sampled around the target region, in this case, the dlPFC. A modelling study by Nieminen and colleagues analyzed different registration methods during neuronavigated TMS and showed that by increasing the number of sampling points, accuracy of landmark-based subject registration can be improved [99].

3.4.3. Coil Calibration

In order for the camera to accurately locate the coil, the setup needs to be precisely calibrated before use. This was done using a pointer with a set of reflective triangulation spheres on the end as well to the dimensions of which the software is precisely calculated. The location of the coil was established by first securely attaching the tracker to the coil in a way that would not interfere with the coil holder, and was not prone to tracker movement, which would render the calibration useless. Subsequently, the pointer was placed into 8 predefined blind holes of a coil attachment. Starting with the slot labeled "1" and moving down in numerical order. The slots were placed at calculated increments around the coil and an in-house developed software allows to obtain the calibration information based on these positions. Precision during this step was crucial as flaws in calibration may cause large discrepancies between the real distances between the subject and the coil and the digital ones, generating imprecision in targeting.

3.4.4. Target Definition

We defined the stimulation target based on the functional connectivity of the brain in a procedure outlined by Cash and colleagues [100]. It has been found that specific parts of the left dlPFC show a high anticorrelation to the sgACC. In previous studies [101, 102] this connectivity pattern of a TMS target was associated with increased clinical response. We use an MNI mask of the sgACC to extract the time course for the voxels within

that mask. After that, we calculated voxelwise correlations with this sgACC timecourse, resulting in an MNI space correlation map which was then transferred back into subject space. Within subject space, we looked at the most anti-correlated point in the left pre-frontal cortex and set that as our target. Oftentimes the most anti-correlated voxel was less accessible due to coil rotation or cortical depth, and therefore, we assessed the five most anti-correlated voxel clusters and selected the most accessible cluster as a target. Using SimNIBS, we then got the optimal coil position based on the anatomy of the head and brain for stimulation, which was then used during the stimulation sessions and adjusted using Brainsight to the best of our abilities, generally staying within 2mm of the target position, within 5 degrees of rotation and tilt.

3.4.5. Dose Adjustment

To account for variations in scalp-cortex distance between motor cortex and the dlPFC, we calculated an adjustment factor for stimulation intensity as suggested by Numssen and colleagues [18]. The scaling factor was acquired based on the sampled coil position from aMT determination in ses-01 and the defined coil position for dlPFC stimulation. We calculated the adjustment factor both using the 99.9th percentile and region of interest (ROI) based comparison and selected the output scaling value, which was closer to the original aMT. Furthermore adjustments were made to account for rounding and subject comfort. We used the equations 3.1 and 3.2 from Numssen and colleagues [18] to get the final stimulation intensity. The intensity calculations and final intensities are presented in Table 3.2.

$$\text{Intensity Scaling Factor} = \frac{\text{E-field at Motor Hotspot (V/m)}}{\text{E-field at Target (V/m)}} \tag{3.1}$$

$$\text{Stimulator Intensity (\%MSO)} = \text{aMT (\%MSO)} * \text{Intensity Scaling Factor} \tag{3.2}$$

3.5. TMS-fMRI

3.5.1. Experimental Setup

The experimental setup, shown in Figure 3.5, was designed to minimize subject motion while allowing for concurrent scanning and stimulation. First, three TIM coil interfaces are plugged into the scanner. Then, a multi-axis fMRI-compatible TMS holder was placed inside the bore of the scanner and fixed using Velcro straps to the TIM coil interfaces. The subject was resting on the scanner bed with their head in the setup. The green mirror mount was lined with pillows to reach the appropriate head height and tilt. The first RF coil was placed on top of the pillows, and then another pillow was placed on top of the coil to increase subject comfort and minimize movement. The stimulation coil was then placed atop the target region, initially just by the experimenter holding the coil to the target. When the correct position, tilt, and rotation were reached, the coil was then fixed using the coil holder. The second coil was placed directly on the right side of the

Subject	ses-01	ses-02	99th	ROI	Scaling	Stimulation Intensity
sub-rel002	50	73	1.1797	1.2084	1.16	85
sub-rel003	49	74	0.9374	1.0482	1.04	77
sub-rel004	47	72	1.3861	1.1579	1.15	83
sub-rel006	53	84	0.9849	0.9444	0.98	83
sub-rel007	53	77	1.0733	1.1166	1.05	81
sub-rel008	43	67	1.1245	1.4287	1.12	75
sub-rel009	54	77	1.0685	1.3153	1.07	83
sub-rel010	50	76	0.9449	0.9609	0.96	73

Table 3.2.: Subjects and their corresponding aMT during the intake session, aMT during ses-02 in the scanner room, the adjustment scaling factors calculated from the 99th percentile and the ROI based scaling factor, and the final stimulation intensity. The scaling Factors are ratios and the stimulation intensities are all in %MSO.

subject's head and fixed using a pillow placed between the coil and the mirror holder; the coil was fixed so that a light pressure was applied to the subject's head to maintain the position of the stimulation coil. If the stimulation coil was moved slightly off target, it was adjusted through the various axes on the coil holder. A mirror was then positioned so that the subject saw the back of the bore of the scanner. Lastly, a screen was placed at the back of the scanner.

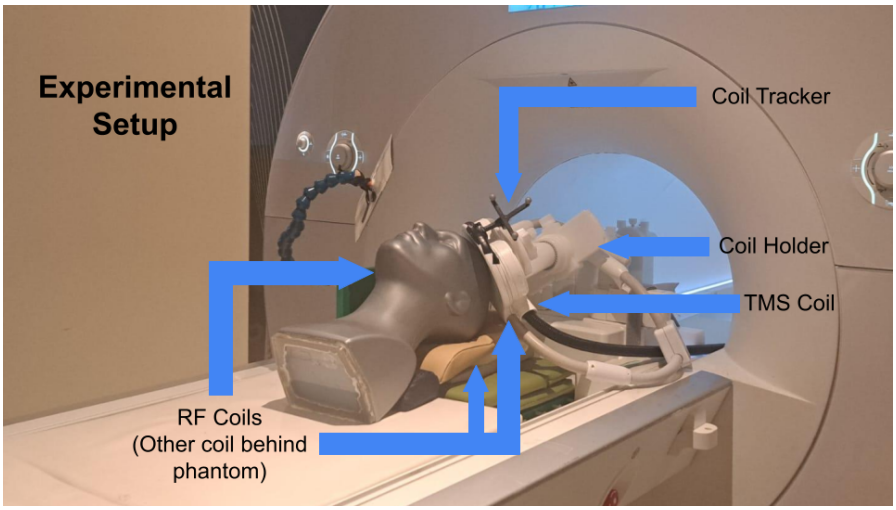

Figure 3.5.: A labeled image of the experimental setup with a phantom subject for reference.

3.5.2. Experimental Design

As we are mainly interested in the immediate effect of stimulation pulses, the stimulation protocol was defined as follows. The stimulation run lasted 500 seconds, during which there were 30 individual stimulations. This means 30 stimulation pulses for singlets and 90 stimulation pulses for triplets. At the start and at the end of the run, there were 20 seconds of baseline, during which no stimulations occurred. The rest of the 460 seconds were split up into 30 randomly timed intervals, with the lowest possible inter-stimulation interval being 10 seconds. This randomization was put in place to avoid the subject from counting between stimulations and confounding the data. An example of the spacing of stimulations is shown in Figure 3.6 below.

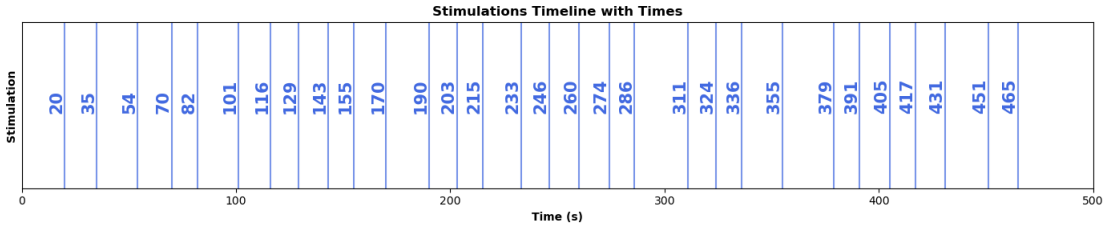

Figure 3.6.: Example of the pseudo-random distribution of TMS pulses throughout the concurrent TMS-fMRI stimulation block.

3.5.3. Imaging Parameters

During the intake session, we first acquired a T1-weighted anatomical scan (MPRAGE, TR=2.1s, TE=3.67ms, flip angle 8°, multiband 4, voxelsize 1x1.016x1.016 mm^3) followed by a resting-state functional scan (CMRR multiband EPI, TR=2s, TE=38ms, flip angle 77°, multiband 4, voxelsize 1.797×1.797×2.0 mm^3) and ended with a T2-weighted anatomical scan (2D TSE, , TR=11.75s, TE=100ms, flip angle 150°, multiband 4, voxelsize 0.859×0.859×2.0 mm^3)

During the stimulation session, we first acquired a resting-state functional scan (CMRR multiband EPI, TR=1s, TE=38ms, flip angle 60°, multiband 4, voxelsize 3.0×3.0 ×3.0 mm^3) followed by a stimulation run (CMRR multiband EPI, TR=1s, TE=38ms, flip angle 60°, multiband 4, voxelsize 3.0×3.0 ×3.0 mm^3). After, we ran another resting-state functional scan, and a stimulation run with the same parameters respectively.

3.5.4. Stimulation Parameters

TMS pulses were triggered using a dedicated software to steer the timing in combination with the MR scanner trigger and an analog AND gate as described in Grosshagauer et al. 2024 [63]. To avoid TMS-induced artifacts, the stimulator used a trigger delay of 80 milliseconds. For singlets, only single biphasic pulses were delivered with each individual trigger. In case of triplets, TMS pulse shape was defined as a biphasic burst, involving 3 pulses at 10 Hz repetition rate.

4. Results

This chapter contains the results acquired from the experiment. It first characterizes the stimulation targets and group-level BOLD activation patterns elicited by the singlet and triplet protocols. It then presents voxel-wise group activation maps and corresponding cluster tables to highlight the spatial extent and statistical significance of these effects. Subject-level activation examples are shown to illustrate individual variability and the typical spatial profile of TMS-evoked responses. Finally, multiple reliability analyses—within-subject, between-subject, and protocol-specific—quantify the consistency of activation patterns across sessions and across individuals.

4.1. Group Level Analysis

The following are BOLD activation maps as a result of stimulation acquired through GLM analysis thresholded to $z > 3.29$ to equate to a $p > 0.001$ significance on a group-level, meaning all subject data combined to show the accumulative effect.

4.1.1. dlPFC Targets

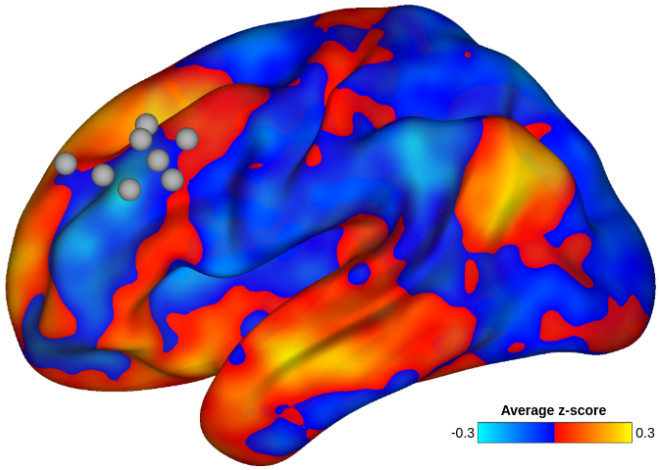

Figure 4.1.: Group-level functional connectivity map of the sgACC averaged across all participants in MNI space, overlaid with the MNI coordinates of each participant's individualized E-field dlPFC hotspot. The individual points represent all of the subjects individual target stimulation sites.

Figure 4.1 shows the average functional connectivity map of the sgACC with points marking the individual dlPFC hotspots used for targeting. The functional connectivity data for this figure comes from the ses-01 intake session. It can be seen that all of the targets lay within the inversely correlated dlPFC area.

4.1.2. Group Level Activation Maps

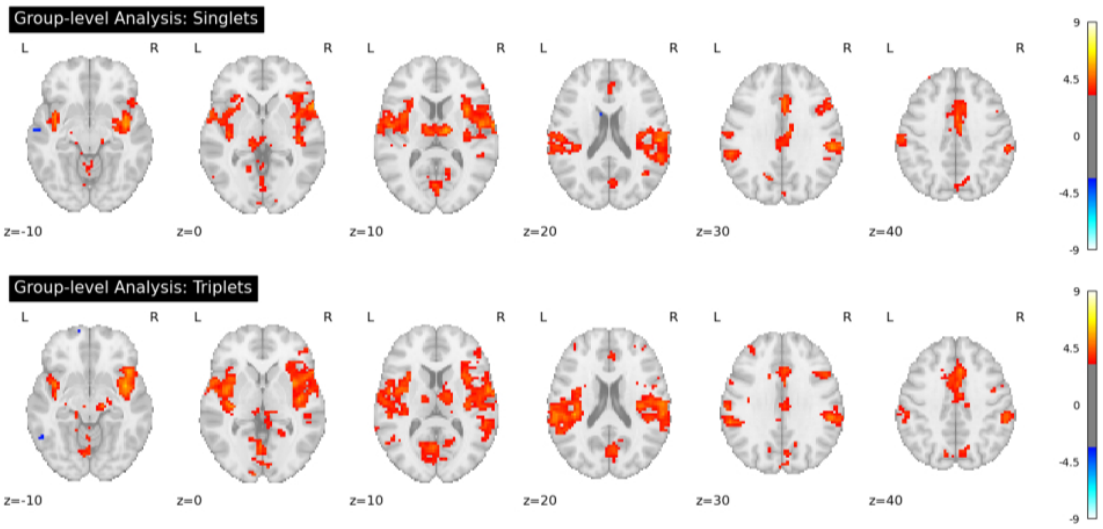

Figure 4.2.: Representative transversal brain slices displaying voxel-wise whole-brain thresholded z-statistic activation maps for the group level activation in singlets (top) and triplets (bottom) fit to a template MNI brain.

The transversal slices depicted in Figure 4.2 show the significant group level activation as a result of stimulation across all subjects for singlets (top) and triplets (bottom). The statistically significant activation clusters for singlets and triplets are presented in Table 4.1 and Table 4.2 respectively. Importantly, the differences in activation patterns between singlets and triplets on a group-level yielded no significant differences.

The transversal brain slices depicted in Figure 4.3 show the corresponding effect sizes of stimulation across all subjects for singlets (top) and triplets (bottom). The red areas show positively correlated activation with respect to the stimulus, whereas blue areas show negative correlations. Subtle inversely correlated effects can be seen in the frontal parts of the singlet activation maps compared to the triplet activation maps (Figure 4.3, slice z=20). A contra-lateral BOLD response can also be observed in the right dlPFC area in singlets which is less focal in triplets.

Region	Hemisphere	X	Y	Z	Peak Z-Stat	Size (cm^3)
Temporal Sup	Left	-42.0	-12.0	-3.00	5.97	28.991
Rolandic Oper	Right	63.0	-18.0	15.75	5.75	40.533
Thalamus	Right	12.0	-12.0	8.25	5.49	5.940
Supp Motor Area	Right	12.0	9.0	49.50	5.12	14.208
Vermis	Bilateral	0.0	-54.0	-3.00	4.81	1.046
Calcarine	Left	0.0	-72.0	12.00	4.61	4.590
Temporal Mid	Right	45.0	-57.0	15.75	4.46	0.708
Frontal Inf Oper	Right	54.0	15.0	30.75	4.19	1.113
Cerebelum	Left	-15.0	-54.0	-21.75	4.17	0.438
Cerebelum	Left	-15.0	-75.0	-18.00	4.08	0.573
Postcentral	Right	27.0	-36.0	72.00	4.05	0.337
Precuneus	Left	0.0	-45.0	60.75	4.02	0.506
Lingual	Right	12.0	-60.0	8.25	3.95	0.438
Lingual	Left	-9.0	-48.0	-3.00	3.92	0.337
Precuneus	Right	12.0	-72.0	42.00	3.90	0.742
Lingual	Left	-18.0	-57.0	0.75	3.77	0.371
Rectus	Left	0.0	36.0	-25.50	-3.70	0.405

Table 4.1.: The z-statistic cluster table for singlet group-level analysis showing the region, hemisphere, coordinates, peak statistic, and size of significant clusters. Anatomical labels were defined using AAL3 atlas [103].

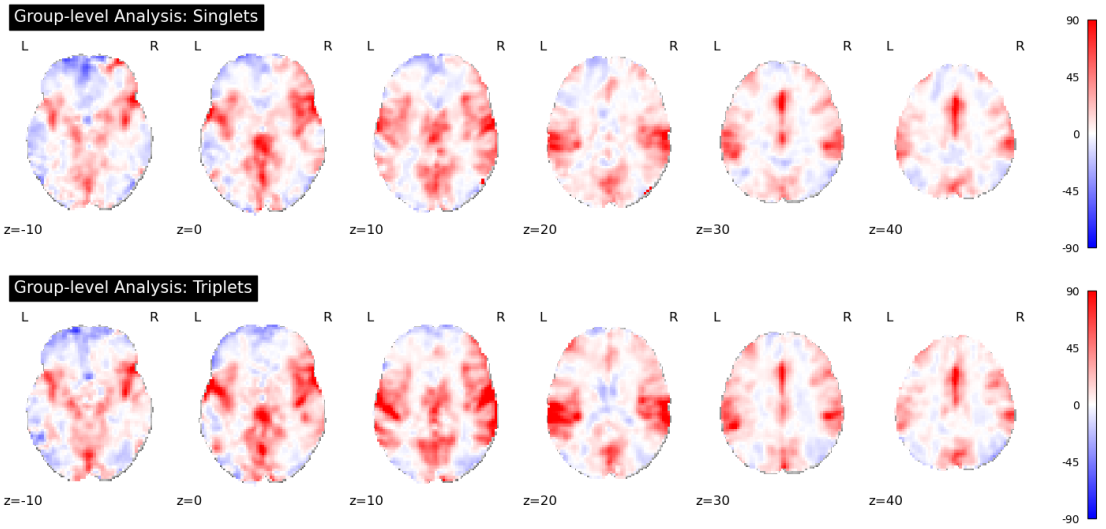

Figure 4.3.: Representative transversal brain slices displaying voxel-wise whole-brain effect size activation maps for the group-level activation in singlets (top) and triplets (bottom) fit to a template MNI brain.

Region	Hemisphere	X	Y	Z	Peak Z-Stat	Size (cm^3)
Insula	Right	42.0	3.0	-10.50	6.10	52.346
Insula	Left	-42.0	-3.0	4.50	5.74	42.018
Cingulum Mid	Right	6.0	21.0	38.25	5.11	16.065
Vermis	Bilateral	0.0	-69.0	-3.00	4.96	15.525
Substantia Nigra	Right	15.0	-21.0	-10.50	4.92	2.025
Thalamus LGN	Left	-27.0	-18.0	-6.75	4.69	0.540
Thalamus	Right	15.0	-9.0	12.00	4.49	2.328
Frontal Inf Oper	Right	51.0	15.0	30.75	4.40	1.080
Frontal Mid	Right	39.0	-3.0	57.00	4.33	1.113
Thalamus	Left	-15.0	-15.0	12.00	4.28	0.877
Precentral	Left	-42.0	-9.0	60.75	4.13	0.641
Thalamus MGN	Left	-12.0	-27.0	-6.75	4.01	0.877
Frontal Mid	Right	51.0	45.0	4.50	3.99	0.911
Vermis	Bilateral	-3.0	-54.0	-10.50	3.82	0.607
Posterior Cingulate	Left	3.0	-33.0	27.00	3.66	0.506
Frontal Mid	Left	-33.0	42.0	30.75	3.63	0.573

Table 4.2.: The z-statistic cluster table for triplet group-level analysis showing the region, hemisphere, coordinates, peak statistic, and size of significant clusters. Anatomical labels were defined using AAL3 atlas [103].

4.2. Subject-Level Analysis

The following are exemplary results of BOLD activation as a result of stimulation acquired through GLM analysis thresholded to $z > 3.29$ to equate to a $p > 0.001$ significance. Only sub-rel006 is shown to exemplify standard activation after stimulation.

Figure 4.4 shows the subject-level activations during each stimulation run for sub-rel006 which showed exemplary activations which represent the types of activation maps that can be seen in other subjects as well as a result of stimulation and different stimulation protocols. From the figure it can be seen that the most consistently active areas are within the auditory and somatosensory areas which are activations that cannot be mitigated due to the sensation of TMS as well as noise of the stimulation itself. Consistently activated areas are also under the stimulation site highlighted by the blue square on top of the brain mosaics. Similar results were found in other subjects and are highlighted by the group-level analysis above.

Figures 4.6 and 4.5 show the effect sizes of each of the 400 parcels during ses-02 (x-axis) in relation to the effect sizes of the same parcels' in ses-03 (y-axis). These graphs show a clear positive correlation between the two sessions demonstrating a inter-session reliability on a single-subject-level in each stimulation protocol. Similar plots for all other subjects can be found in the Appendix.

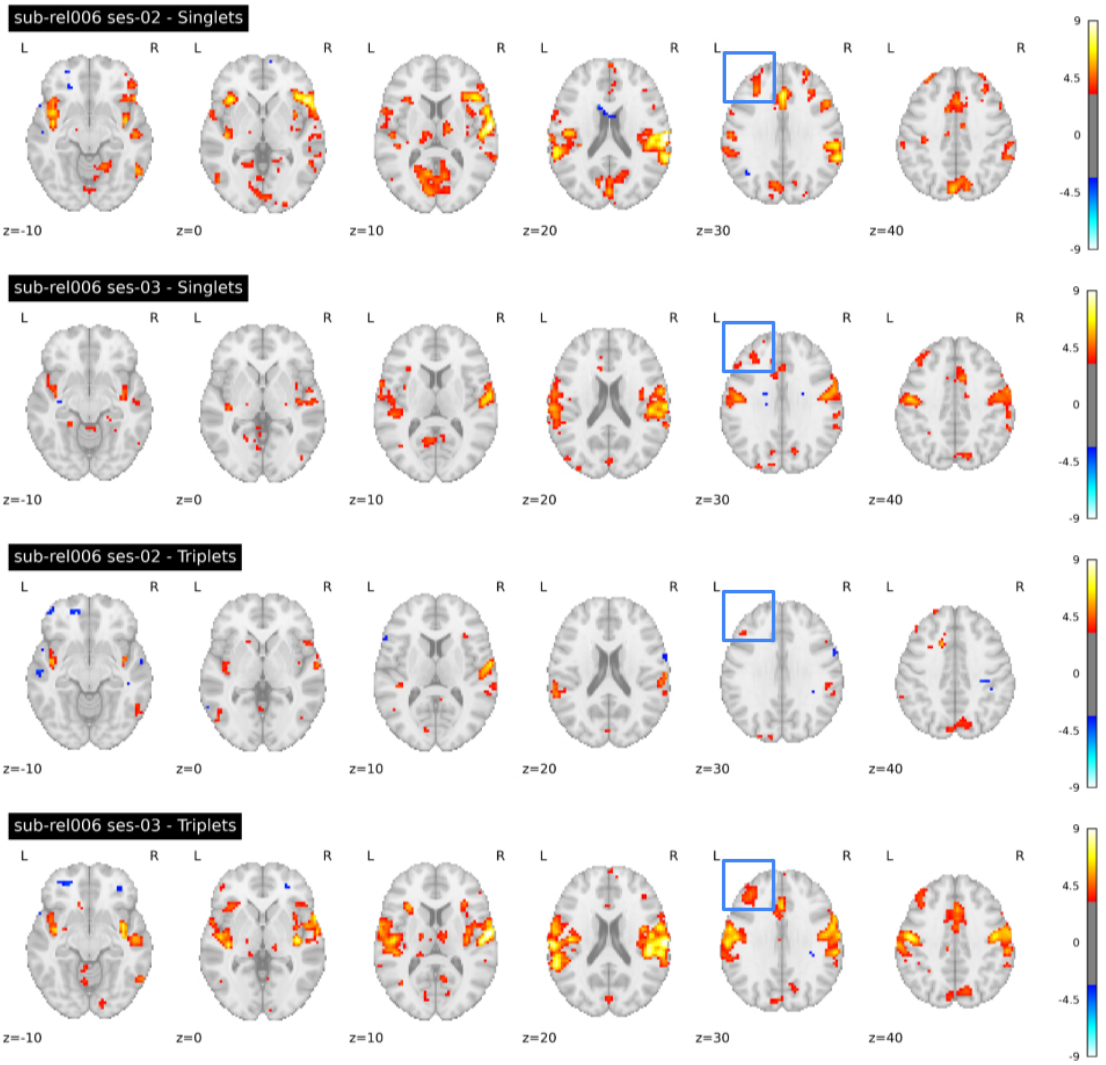

Figure 4.4.: Representative transversal brain slices displaying voxel-wise whole-brain thresholded z-statistic activation maps for subject sub-rel006 during the singlets protocol in ses-02 and ses-03 (top 2 respectively) and singlets protocol in ses-02 and ses-03 (bottom 2 respectively) fit to a template MNI brain. The approximate location of the stimulation site is highlighted in the blue square.

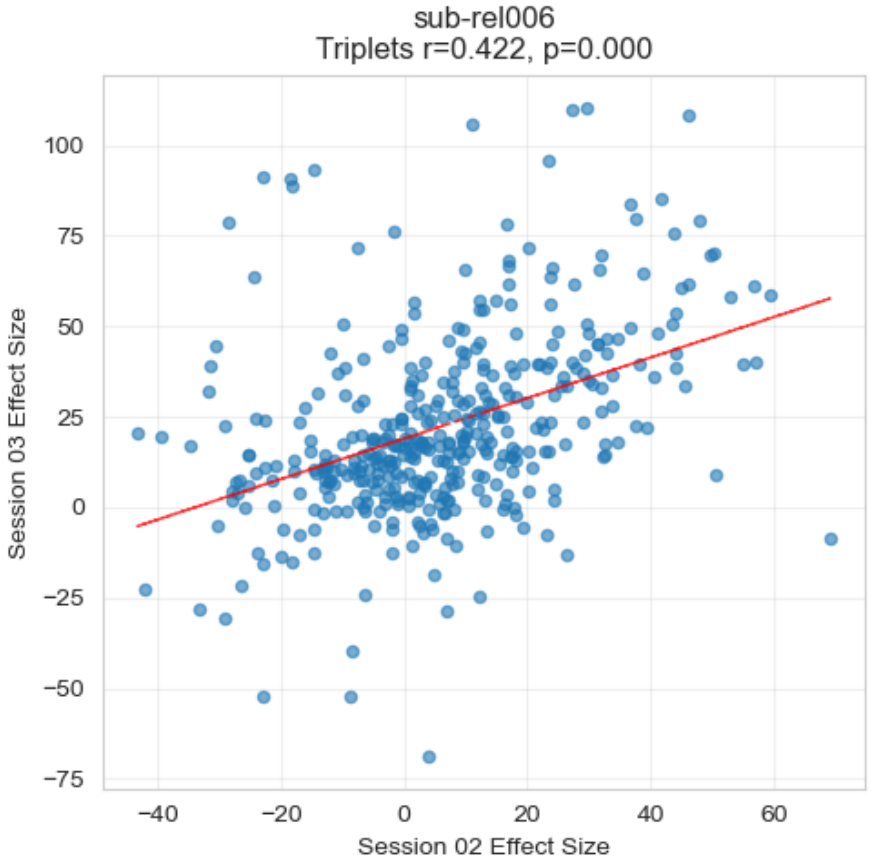

Figure 4.5.: Parcel-wise correspondence of singlet-evoked BOLD effect sizes across sessions for participant sub-rel006. Each point represents a cortical parcel, plotting its effect size in ses-02 against ses-03. The red regression line illustrates the positive correlation between sessions.

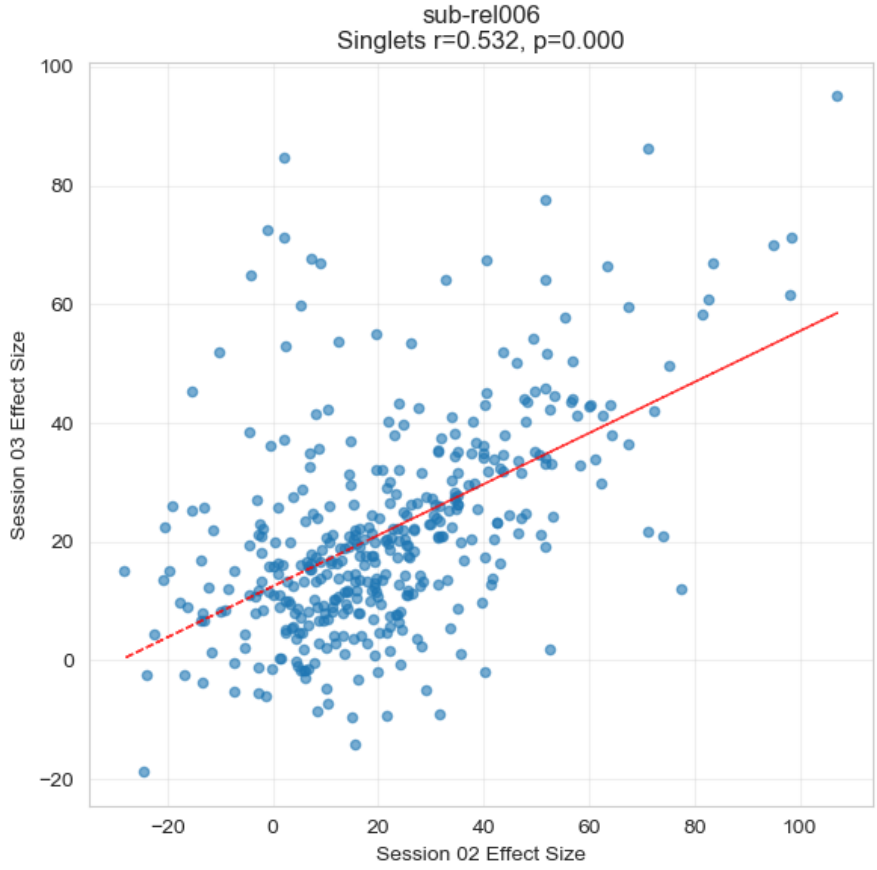

Figure 4.6.: Parcel-wise correspondence of triplet-evoked BOLD effect sizes across sessions for participant sub-rel006. Each point represents a cortical parcel, plotting its effect size in ses-02 against ses-03. The red regression line illustrates the positive correlation between sessions.

4.3. Reliability Analysis

In this section, the investigations on reliability of stimulation protocols and all corresponding analysis are presented. The results shown were obtained by calculating Pearson's correlations of all of the parcels within the Schaefer atlases, a commonly used brain parcelation method [95], between ses-02 and ses-03.

4.3.1. Group Reliability

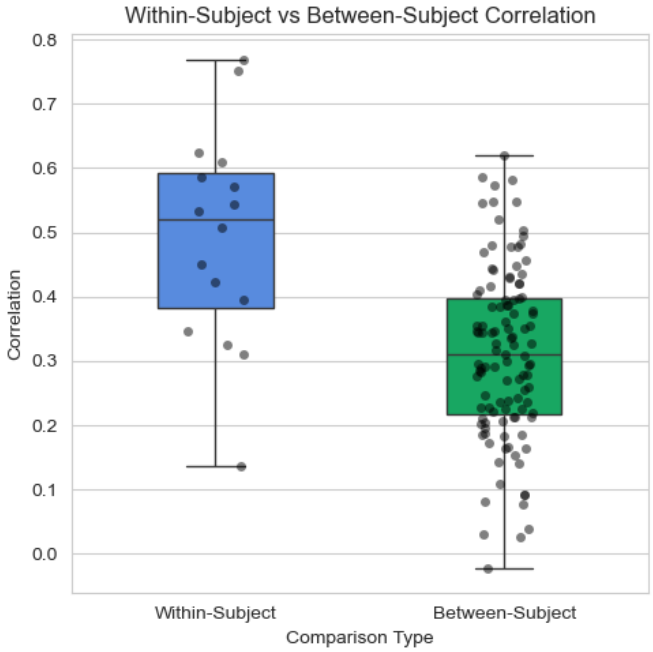

Figure 4.7.: Comparison of within-subject and between-subject reliability in TMS-evoked BOLD activation patterns. Boxplots show the distribution of Pearson correlations for session-to-session reliability within subject (left) and similarity across different subjects (right). Individual data points represent correlations for each subject or subject pair.

Figure 4.7 displays the correlations between ses-02 and ses-03 within the same subject and across all subject combinations. From the figure it can be seen that within-subject correlations are higher (mean=0.493, SD=0.162) than the between-subject correlations (mean=0.311, SD=0.133). The individual points on the box plots represent the data points from which the boxplot is graphed. A paired t-test resulted in the following values: t = 3.755, p = 0.002. This graph represents both the singlet and triplet protocols combined.

Figure 4.8 shows the difference in reliability within and between subjects across sessions respective to the stimulation protocol of use. From the graph it can be seen that the

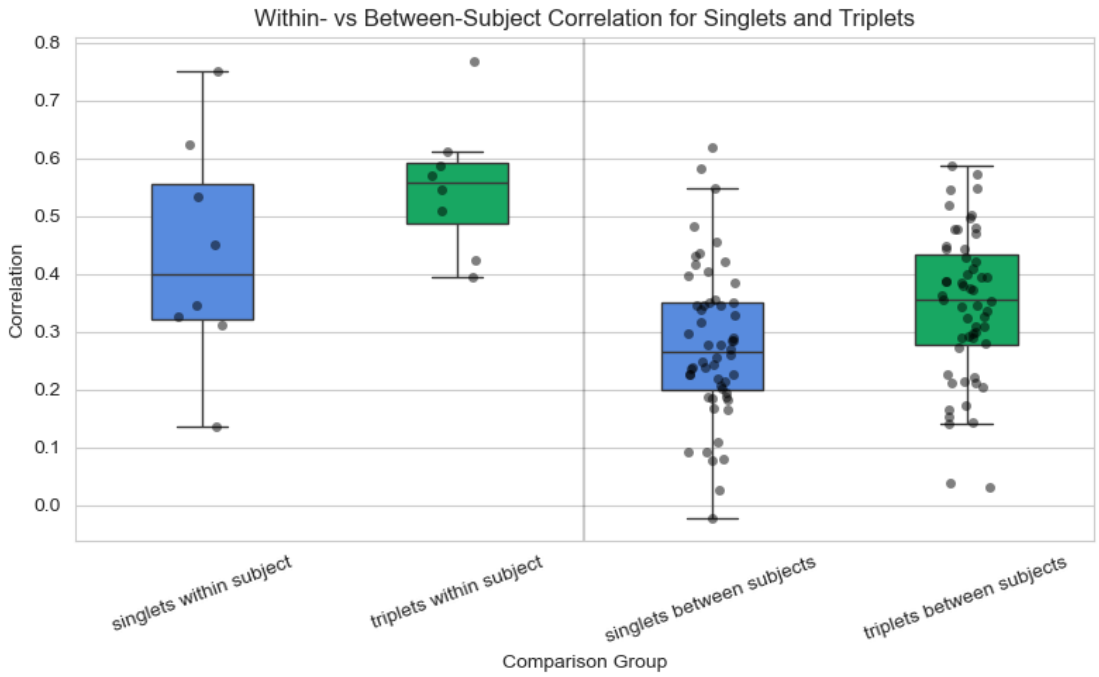

Figure 4.8.: Comparison of singlets and triplets in within- and between-subject correlations across all parcels across ses-02 and ses-03. Individual data points represent correlations for each subject or subject pair. The blue bars represent singlets and the green bars represent triplets.

triplets protocol has a higher correlation (mean=0.551, SD=0.109) across sessions than the singlet stimulation protocol (mean=0.435, SD=0.183). Both singlets (mean=0.278, SD=0.131) and triplets (mean=0.344, SD=0.127) show lower reliability between subject than within subject.

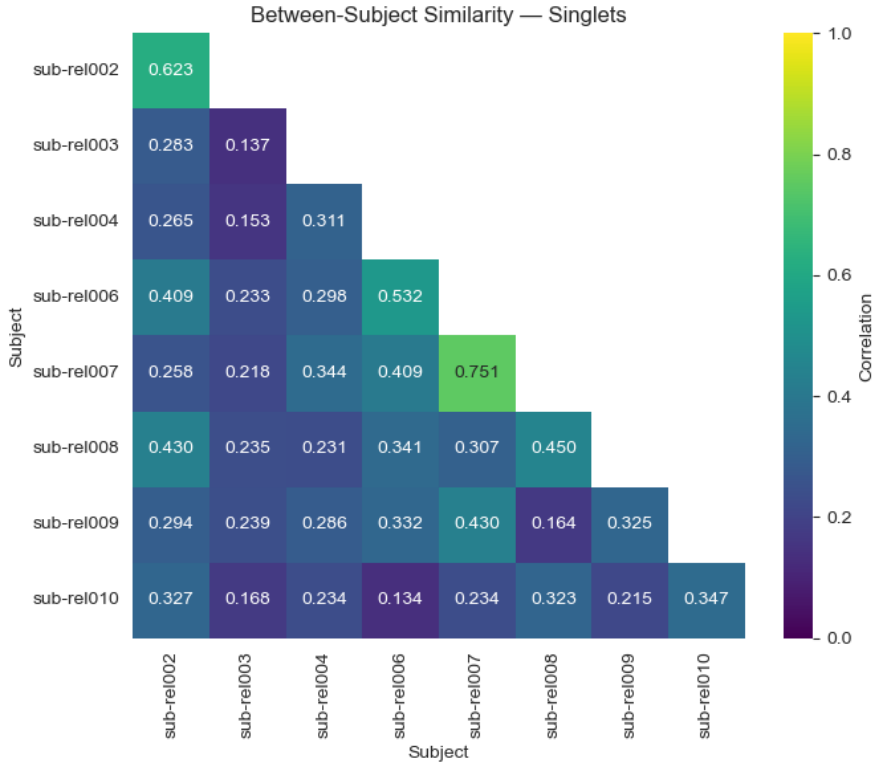

Figure 4.9.: Correlation matrix showing between- and within-subject similarity of singlet-evoked BOLD response patterns. The lower-triangular heatmap shows Pearson correlations between effect-size maps averaged across protocols and sessions for every pair of participants. Diagonal values represent each participant's mean within-subject cross-session reliability. The blue bars represent singlets and the green bars represent triplets.

Figures 4.9 and 4.10 show the subject x subject similarity matrix for singlets and triplets respectively. The values underneath the diagonal represent between subject correlation and the diagonal values represent the within subject correlation. It can be seen that the values along the diagonal are higher. It is important to note that one parcel (Right Hemisphere Visual 22 230) for sub-rel003 ses-02 singlets has an inconsistently large effect size. The same goes for sub-rel008 ses-02 singlets where one parcel (Right Hemisphere Salience/Ventral Attention Med 8 317) has an inconsistently high negative effect size and would also be considered an outlier. These outliers significantly reduce the correlation of singlets arcoss sessions in the two subjects. We chose to include these outliers in the data

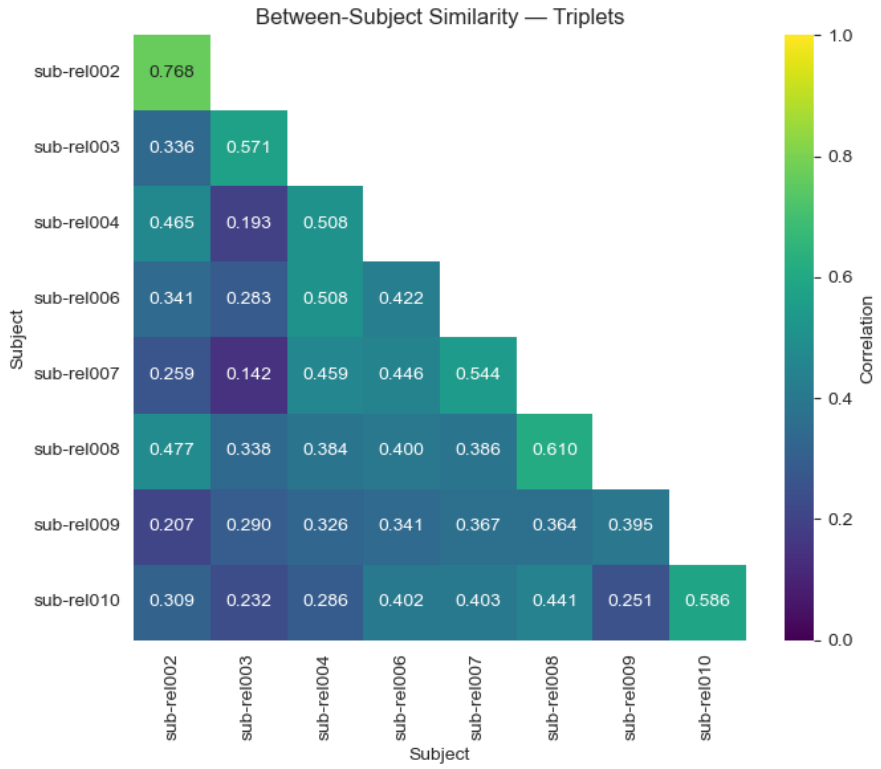

Figure 4.10.: Correlation matrix showing between- and within-subject similarity of triplet-evoked BOLD response patterns. The lower-triangular heatmap shows Pearson correlations between effect-size maps averaged across protocols and sessions for every pair of participants. Diagonal values represent each participant's mean within-subject cross-session reliability.

to maintain consistency between subjects.

4.3.2. Network-Level Reliability

The following is a parcel-wise network level analysis of the effect sizes and correlations across subjects. Networks were assigned to each parcel of the Schäfer parcellation [95] based on the Yeo networks [96].

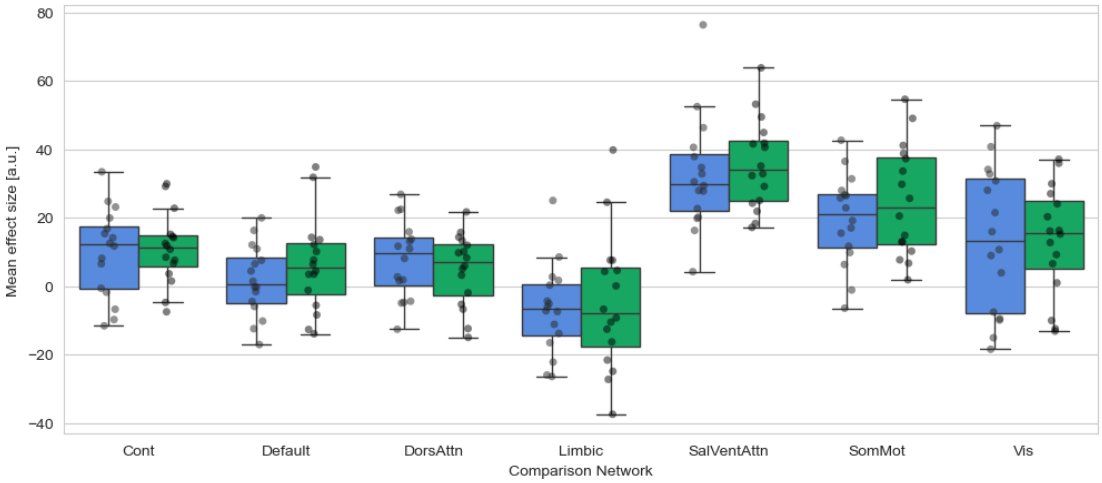

Figure 4.11.: Box and whisker plots showing effect sizes of parcels divided into their respective functional networks in arbitrary units (a.u.). The selected networks are based on the Schaefer atlases [95] and the seven Yeo networks [96]. The parcel categories are: Control, Default Mode, Dorsal Attention, Limbic, Salience/Ventral Attention, Somatomotor, and Visual Network respectively. The blue bars represent singlets and the green bars represent triplets.

Figure 4.11 shows the network-level effect sizes of singlets and triplets grouped by functional network. This analysis revealed the network-specific effect sizes shown in Table 4.3 The Salience/Ventral Attention, Somatomotor, and Visual networks show the highest effect size and the Control, Default Mode, Dorsal Attention, and Limbic networks display a lower effect size but generally less variability.

Figure 4.12 shows the network-level correlations of singlets and triplets grouped by functional networks. This analysis revealed the network-specific correlations shown in Table 4.3. The Somatomotor and Salience/Ventral Attention networks show the highest correlations followed by the Control and Default Mode Networks, and lastly the Dorsal Attention, Limbic, and Visual networks show the lowest correlations with the highest variability.

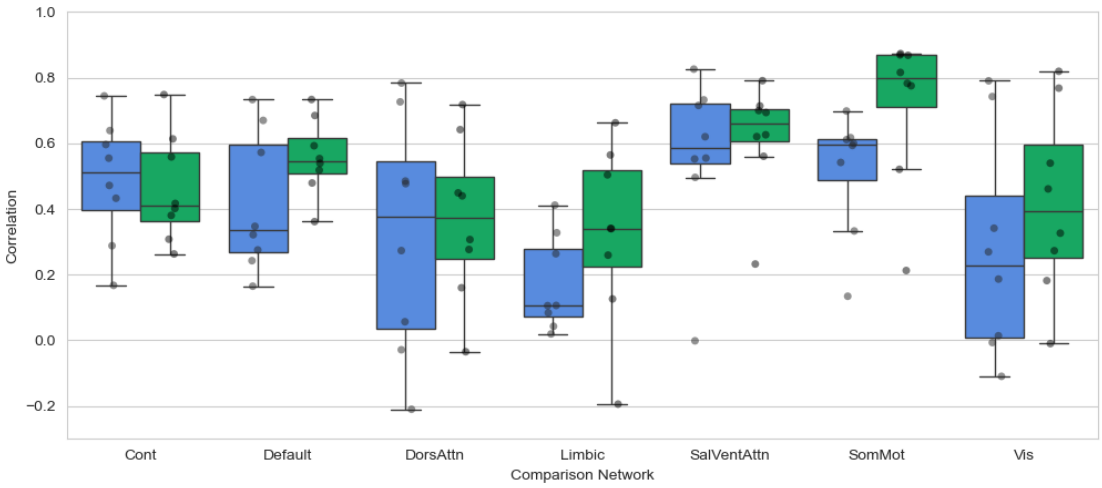

Figure 4.12.: Box and whisker plots showing the correlation of parcels divided into their respective functional networks between ses-02 and ses-03. The selected networks are based on the Schaefer atlases [95] and the seven Yeo networks [96]. The parcel categories are: Control, Default Mode, Dorsal Attention, Limbic, Salience/Ventral Attention, Somatomotor, and Visual Network respectively. The blue bars represent singlets and the green bars represent triplets.

Network	**Protocol**	**Effect Size μ/SD**	**Correlation μ/SD**
Control	Singlets	9.761/12.598	0.487/0.177
	Triplets	11.036/10.123	0.461/0.154
Default Mode	Singlets	1.693/10.030	0.416/0.199
	Triplets	6.291/13.303	0.558/0.109
Dorsal Attention	Singlets	7.785/10.951	0.320/0.336
	Triplets	4.886/10.165	0.370/0.231
Limbic	Singlets	-6.728/12.793	0.170/0.135
	Triplets	-4.860/19.115	0.325/0.254
Salience / Ventral Attention	Singlets	32.493/16.081	0.562/0.236
	Triplets	35.706/12.764	0.617/0.159
Somatomotor	Singlets	19.516/12.828	0.516/0.175
	Triplets	24.853/15.708	0.715/0.218
Visual	Singlets	13.368/20.471	0.278/0.314
	Triplets	13.497/15.499	0.420/0.266

Table 4.3.: Mean and standard deviation for each network (Control, Default Mode, Dorsal Attention, Limbic, Salience/Ventral Attention, Somatomotor, and Visual), for each protocol (singlets and triplets), and for both effect size and correlation. The table is a supplement to the Figures 4.11 and 4.12.

5. Discussion

The following chapter is a discussion on the findings and their implications for both the technology of TMS, its use in clinics and research labs, and the greater cognitive science discussion. The chapter also discusses the study's limitations.

5.1. Results

Within this study, we compared BOLD responses to different TMS protocols across sessions and subjects. On a group-level very few differences were observed between the two stimulation protocols suggesting that they engage similar brain networks. On a subject-level we saw highly similar activation maps across sessions, which, however, were highly subject specific. In terms of the reliability the data show: within-subject reliability is higher than between-subject reliability and activation maps from triplets are more reliable than from singlets. This finding is consistent across various functional brain networks.

5.1.1. Group-Level Activation

Overall group-level activations show similar patters to previously published TMS-fMRI data in both singlets [62] and triplets [63]. As seen in Tables 4.1 and 4.2 we observed major activation in the thalamus and insula which are regions often associated with hearing, sensation, and pain perception. The TMS-induced activation within these areas is difficult to discriminate from the indirect stimulation effects suggesting careful interpretation of these findings. On a group-level we observed that both singlets and triplets elicit very similar activation patterns in the brain, resulting in no statistically significant differences. The effect sizes show similar network engagement. On a voxel level singlets showed slightly stronger bilateral activation of the dlPFC and inhibition in the surrounding regions which was not present in triplets as seen in Figure 4.3. Differences between protocols were mostly in terms of effect size rather than activation patterns, suggesting that triplets activate the same networks but with a higher effect size. Application of multiple pulses compared to single pulses may still yield different results in other brain regions, as shown in results observed in paired pulses in previous literature [23]. We did not observe such inhibitory effects in the dlPFC, but rather a stronger BOLD response.

5.1.2. Subject-Level Activation

On a subject-level we see comparable activities in each participant. The main activation we see is somatomotor activation as seen by Figure 4.4. This is likely caused by scalp

sensation of the stimulation and the clicking noise it makes conducted both through air and bone. These sensory effects are, however, hard to mitigate in concurrent TMS-fMRI research as sham stimulation would be required and current hardware does not replicate the sensation of TMS exactly. All subjects had a positive parcel-wise correlation between both sessions suggesting inter-session reliability of TMS evoked BOLD signal. An interesting effect can be observed by comparing the significant activations between the first and second stimulation run within one session. We consistently observed lower activations in the second stimulation run suggesting a habituation effect within a session. As the subject got more accustomed to the setup and environment, the sensations caused lower BOLD activations. Nonetheless, significant activations within the dlPFC and other brain regions areas were still present suggesting successful stimulation. Due to the continuous use of neuronavigation during scanning, movement effects can be excluded as causes for these effects. Similarly, meticulous care was taken during coil position prior to and during all scans, which is a precaution not commonly conducted during TMS-fMRI studies. Thus, online neuonavigation is an aspect of TMS-fMRI that should be considered for all future studies.

5.1.3. Reliability

The primary finding of this study lies within the reliability within and between subjects and the reliability of the two stimulation protocols. From Figure 4.7 it can be seen that within subject parcel-wise correlations are higher than the between subject comparison. This effect is observed in both singlets and triplets as seen in Figure 4.8. This confirms the idea that individual anatomical and functional connectivity differences greatly impact the amplitude and position of the activations caused by TMS. The finding reaffirms the necessity for individualized stimulation procedures due to the between subject differences in functional connectivity based stimulation target and cautions over generalizations for group-level analysis due to the effect outcomes.

We found that triplets have higher reliability across stimulation sessions conmpared to singlets, suggesting that the choice of stimulation protocol has an effect on the consistency of stimulation-related BOLD response. This can be seen in Figure 4.8. This effect is true for both within-subject and across-subject reliability, with triplets showing higher means in both cases. This is an important finding that implies that single pulse designs might not be sensitive enough to reveal activation patterns. The lower reliability of singlets compared to triplets informs future experimental design. Using multi-pulse stimulation in TMS-fMRI studies might increase the validity and longitudinal implications of research studies, due to the higher reliability in BOLD responses.

5.1.4. Network-Level Reliability

The results of the network-level analysis of effect sizes shown in Figure 4.11 suggest the following findings. The salience/ventral attention and somatomotor networks show the highest effect sizes for both protocols with slight increases for triplets. This higher effect size may be due to the unspecific side effects of the sensation of TMS as the sensations of

stimulation show in these networks. Conversely, the default mode and dorsal attention networks showed the lowest effect sizes and low variability. Interestingly, the limbic network showed a negative effect size suggesting inhibition in the associated areas, but also showed higher variability; importantly the sgACC is associated with this network.

The network-level analysis of correlations shown in Figure 4.12 suggests the following. The salience/ventral attention and somatomotor networks had the highest reliability across session with the somatomotor network having a clear difference in correlation between protocols. Triplets showed a much higher similarity than singlets, but this may be an effect of the ordering of stimulation runs combined with the subjects' habituation to the setup and stimulation throughout individual stimulation sessions. Mitigation of this confound is difficult as it directly conflicts with the order effect and motion confounds as we wanted to assure the protocols do not confound each others and that the subjects are not startled as a result of their very first TMS-fMRI stimulation causing movement. The limbic network shows a generally low similarity across sessions but a clear difference in reliability between protocols with lower reliability for singlets; the higher reliability for triplets is, however, highly variable. The generally lower values may be due to the network being in regions with lower signal due to inherent RF coil placement.

Comparison of correlation and effect size from Table 4.3 revealed that triplets showed stronger somatomotor activation which is also associated with higher correlation values compared to singlets. This suggests a robust and reliable activation in somatomotor areas. Singlets compared to triplets showed stronger inhibition in the limbic network, but also showed low correlation across sessions. This might hint towards protocol-specific effects in the limbic network which the sgACC is often attributed to. Therefore, further research would be needed to confirm whether sgACC deactivation can be influenced by stimulation protocol. The default mode network showed greater activation in triplets with higher reliability compared to singlets, showing that using triplets may more effectively engage frontal cortical regions.

In summary, the findings show an overall comparably high reliability of TMS-related BOLD response, but with significant inter-individual variance. Reliability is also network-specific as well as protocol-specific.

5.1.5. Implications for TMS Use

Currently, TMS is widely used in both research facilities and clinics across the world for exploring and exploiting non-invasive brain stimulation. Concurrent TMS-fMRI allows researchers to causally probe specific brain regions and observe their effects on ROI and network-level brain activation as well as behavior. Little is known about the reliability of this method across different time points however. A previous study by Hawco and colleagues demonstrated high within-run reliability [8] but a longitudinal study has not yet been conducted. Thus, this study investigated whether TMS induced a reliable BOLD response across sessions. The findings of this study are relevant for research use as it provides important information for design of future studies. If a specific cortical target is used and is meticulously targeted on different days, then it can be expected to activate the brain in highly similar but not perfectly identical ways. Future studies would need to

be conducted to determine whether this finding generalizes beyond the dlPFC as in this study, we stimulated a very precise region and other cortical areas may exhibit different response patterns. This study suggests that triplets are more reliable in the response they elicit, providing insights into the necessity to consider the protocol of stimulation, as single pulses might create less reliable BOLD responses across sessions, which might affect the interpretation of TMS-fMRI outcomes. While the finding that within-subject reliability is much higher than between-subject is not unexpected, due to the personalized targeting and dosing, it confirms that inter-individual variability is high and can decrease group-level results. Thus, in addition to group-level, TMS-fMRI results should always be investigated on the subject-level. All of these findings support the consistency and reliability of TMS-fMRI, supporting its use in research and clinics.

5.1.6. Implications for Cognitive Science

A common assumption within cognitive science in the stability of the brain behaviors. Since the brain is the substrate that drives cognition, the fundamental phenomena it exhibits inform cognitive modeling and experimental design. Because of this, the assumptions that are made need to be empirically tested to validate the outcomes. This assumption can directly be tested by TMS-fMRI as it allows for causal probing and observation of brain region and network activation over time.

The findings of this TMS-fMRI study corroborate the assumption that the responses of the brain to specific stimulation are consistent over a specific time scale. Thus, these reliability findings can be extrapolated onto the ways in which natural stimuli elicit neural activation. Of course, natural stimuli are much less controlled and not artificially induced, putting a lot of value on the context within which the stimulus occurs enforcing the ideas of 4E cognition. If a study design would allow for the conditions to match precisely across different days, then it would not be hard to imagine how across session reliability at different time points could be achieved. However, caution needs to be taken in interpreting this finding as it uses a very specific method of elucidating brain activation. These extrapolations are, of course, highly speculative but the findings provide a stepping stone into a deeper understanding of reliability and reproducibility which is an often undermined aspect of neuroscience.

5.2. Limitations

Despite the strengths of this study, some limitations need to be acknowledged. The most significant constraint is the small sample size, which reflects the practical difficulty of acquiring concurrent TMS–fMRI data across multiple sessions. Due to the difficult preparation, individualized methodology, long scanning time, and the chances of data-corrupting errors being quite high, the number of fully collected datasets is limited. This reduces statistical power primarily on a group level and may obscure subtle effects. As a result, the generalization of the findings should be interpreted carefully.

A second limitation concerns the indirect nature of the BOLD signal. fMRI measures

changes in blood flow rather than neural activity itself. Although neurovascular coupling is robust, it is still an inference about the underlying neuronal processes. As a result, any conclusions about network or regional activation must acknowledge that the measured signal is a proxy, and not a direct readout of neural activity. On a similar note, the study assumes that motor-threshold stimulation intensity generalizes to other cortical areas. This is a standard assumption in TMS research as non-motor regions lack physiological validation cues. The true stimulation threshold of dlPFC cannot be directly measured, and E-field simulations preformed with SimNIBS can only approximate electric field distributions in tissue, but do not tell us anything about the actual activation patterns. This matters because individual brain region differences may cause identical stimulation percentages to impact different neuronal populations at diverging levels. This, however, is an aspect of TMS research that currently cannot be mitigated.

A further limitation is that perfect session-to-session consistency cannot be achieved. Factors such as sleep, caffeine intake, stress, and time of day can alter cortical excitability. These factors cannot be fully controlled by the researcher. Achieving perfect stimulation precision is impossible with current TMS–fMRI hardware. Small coil-position shifts, like those caused by startle responses to the first pulse, introduce imprecision that is difficult to avoid despite careful preventative measures such as online neuronavigation. These movements, even though they are often sub-millimeter, are meaningful because they can shift the stimulation site from a gyral crown into a sulcal wall or vice versa, resulting in different E-field distributions and potentially different activation patterns. Another setup limitation is the fact that perfect RF coil placement on different scanning days is impossible as the position of the RF coils could not be consistently tracked across sessions. This may have caused different signal levels in the same brain regions on different days.

6. Conclusion

The findings of this study suggest that TMS-fMRI is a reliable method for investigating stimulation-induced brain activity in the dlPFC and associated networks. Given that coil positioning is accurate and consistent and a proper stimulation protocol is selected based on the target of which activation is to be altered stimulation consistently elicited activations across session. With no inherent effect differences between singlets and triplets the results suggest that triplets are better than singlets for eliciting a more consistent response across sessions as well as across participants. The findings further showed significant inter-individual variability, which was reduced by using triplets. These findings have implications for the future of both clinical and research applications.

In research uses, singlets stimulation protocols are commonly used to investigate TMS-induced BOLD response. We, however, found that triplets produce a stronger and more reliable response during stimulation. While multi-pulse stimulations are more uncomfortable for the subject, they might be necessary to obtain reliable BOLD activation patterns, as they engage specific ROIs and associated functional networks with higher similarity across sessions. However, it remains unclear whether network effects are exactly identical; in our sample, the statistical power was likely too low to detect more subtle protocol-specific differences.

With TMS-fMRI being increasingly used to probe brain response to TMS also in clinical cohorts, the selection of optimal protocols to detect target engagement is an open question. Based on the findings of this thesis, the BOLD response induced by singlets is not strong enough to yield reliable results with the small group sizes used, especially across sessions. Therefore, using triplets could provide more reliable insights. In parallel, we showed that strong inter-session similarity can be achieved, if steps are taken to ensure a high degree of targeting precision. If recruitment of the same target region is desired by clinicians during treatment then proper care needs to be taken during targeting and throughout the stimulation to elicit activation in the desired brain regions.

Further research is needed to reaffirm these findings for investigating different aspects of brain stimulation. This study focused on dlPFC stimulation, and extrapolating these findings to other brain regions may not be accurate as they may show different responses to the tested protocols. Similarly, the conclusions drawn from this study should be interpreted lightly due to the small sample size urging researchers to expand this study onto a larger subject population.

Bibliography

[1] Francisco J. Varela, Eleanor Rosch, and Evan Thompson. *The Embodied Mind: Cognitive Science and Human Experience*. The MIT Press, September 1991.

[2] A.T. Barker, R. Jalinous, and I.L. Freeston. Non-invasive magnetic stimulation of human motor cortex. *The Lancet*, 325(8437):1106–1107, May 1985.

[3] World Health Organization. Depressive disorder (depression), March 2023.

[4] Daphne Voineskos, Zafiris J Daskalakis, and Daniel M. Blumberger. Management of treatment-resistant depression: Challenges and strategies. *Neuropsychiatric Disease and Treatment*, Volume 16:221–234, January 2020.

[5] RajivKumar Saini, Amit Chail, PS Bhat, Kalpana Srivastava, and Vinay Chauhan. Transcranial magnetic stimulation: A review of its evolution and current applications. *Industrial Psychiatry Journal*, 27(2):172, 2018.

[6] Benjamin D. Greenberg, Mark S. George, Jonathan Martin, Juliet D.and Benjamin, Thomas E. Schlaepfer, Margaret Altemus, Eric M. Wassermann, Robert M. Post, and Dennis L. Murphy. Effect of prefrontal repetitive transcranial magnetic stimulation in obsessive-compulsive disorder: a preliminary study. *American Journal of Psychiatry*, 154(6):867–869, June 1997.

[7] Dean Walton, David C Spencer, Sarah J. Nevitt, and Benedict Daniel Michael. Transcranial magnetic stimulation for the treatment of epilepsy. *The Cochrane database of systematic reviews*, 4:CD011025, 2021.

[8] Colin Hawco, Jennifer K. E. Steeves, Aristotle N. Voineskos, Daniel M. Blumberger, and Zafiris J. Daskalakis. Within-subject reliability of concurrent tms-fmri during a single session. *Psychophysiology*, 60(7):e14252, 2023. e14252 PsyP-2021-0556.R2.

[9] Russell A. Poldrack, Timothy O. Laumann, Oluwasanmi Koyejo, Brenda Gregory, Ashleigh Hover, Mei-Yen Chen, Krzysztof J. Gorgolewski, Jeffrey Luci, Sung Jun Joo, Ryan L. Boyd, Scott Hunicke-Smith, Zack Booth Simpson, Thomas Caven, Vanessa Sochat, James M. Shine, Evan Gordon, Abraham Z. Snyder, Babatunde Adeyemo, Steven E. Petersen, David C. Glahn, D. Reese Mckay, Joanne E. Curran, Harald H. H. Göring, Melanie A. Carless, John Blangero, Robert Dougherty, Alexander Leemans, Daniel A. Handwerker, Laurie Frick, Edward M. Marcotte, and Jeanette A. Mumford. Long-term neural and physiological phenotyping of a single human. *Nature Communications*, 6(1), December 2015.

[10] Axel Thielscher, Andre Antunes, and Guilherme B. Saturnino. Field modeling for transcranial magnetic stimulation: A useful tool to understand the physiological effects of tms? In *2015 37th Annual International Conference of the IEEE Engineering in Medicine and Biology Society (EMBC)*, pages 222–225. IEEE, August 2015.

[11] Simone Rossi, Andrea Antal, Sven Bestmann, Marom Bikson, Carmen Brewer, Jürgen Brockmöller, Linda L. Carpenter, Massimo Cincotta, Robert Chen, Jeff D. Daskalakis, Vincenzo Di Lazzaro, Michael D. Fox, Mark S. George, Donald Gilbert, Vasilios K. Kimiskidis, Giacomo Koch, Risto J. Ilmoniemi, Jean Pascal Lefaucheur, Letizia Leocani, Sarah H. Lisanby, Carlo Miniussi, Frank Padberg, Alvaro Pascual-Leone, Walter Paulus, Angel V. Peterchev, Angelo Quartarone, Alexander Rotenberg, John Rothwell, Paolo M. Rossini, Emiliano Santarnecchi, Mouhsin M. Shafi, Hartwig R. Siebner, Yoshikatzu Ugawa, Eric M. Wassermann, Abraham Zangen, Ulf Ziemann, and Mark Hallett. Safety and recommendations for tms use in healthy subjects and patient populations, with updates on training, ethical and regulatory issues: Expert guidelines. *Clinical Neurophysiology*, 132(1):269–306, 2021.

[12] Tom Dufor, Ann M. Lohof, and Rachel M. Sherrard. Magnetic stimulation as a therapeutic approach for brain modulation and repair: Underlying molecular and cellular mechanisms. *International Journal of Molecular Sciences*, 24(22), 2023.

[13] S. Ueno, T. Tashiro, and K. Harada. Localized stimulation of neural tissues in the brain by means of a paired configuration of time-varying magnetic fields. *Journal of Applied Physics*, 64(10):5862–5864, November 1988.

[14] Maria Drakaki, Claus Mathiesen, Hartwig R. Siebner, Kristoffer Madsen, and Axel Thielscher. Database of 25 validated coil models for electric field simulations for tms. *Brain Stimulation*, 15(3):697–706, 2022.

[15] Hartwig R. Siebner, Klaus Funke, Aman S. Aberra, Andrea Antal, Sven Bestmann, Robert Chen, Joseph Classen, Marco Davare, Vincenzo Di Lazzaro, Peter T. Fox, Mark Hallett, Anke N. Karabanov, Janine Kesselheim, Mikkel M. Beck, Giacomo Koch, David Liebetanz, Sabine Meunier, Carlo Miniussi, Walter Paulus, Angel V. Peterchev, Traian Popa, Michael C. Ridding, Axel Thielscher, Ulf Ziemann, John C. Rothwell, and Yoshikazu Ugawa. Transcranial magnetic stimulation of the brain: What is stimulated? – a consensus and critical position paper. *Clinical Neurophysiology*, 140:59–97, 2022.

[16] Oula Puonti, Koen Van Leemput, Guilherme B. Saturnino, Hartwig R. Siebner, Kristoffer H. Madsen, and Axel Thielscher. Accurate and robust whole-head segmentation from magnetic resonance images for individualized head modeling. *NeuroImage*, 219:117044, 2020.

[17] Alexander Opitz, Mirko Windhoff, Robin M. Heidemann, Robert Turner, and Axel Thielscher. How the brain tissue shapes the electric field induced by transcranial magnetic stimulation. *NeuroImage*, 58(3):849–859, 2011.

[18] Ole Numssen, Philipp Kuhnke, Konstantin Weise, and Gesa Hartwigsen. Electric-field-based dosing for tms. *Imaging Neuroscience*, 2:1–12, March 2024.

[19] Gonçalo Cotovio, Fabiana Ventura, Daniel Rodrigues da Silva, Patrícia Pereira, and Albino J. Oliveira-Maia. Regulatory clearance and approval of therapeutic protocols of transcranial magnetic stimulation for psychiatric disorders. *Brain Sciences*, 13(7):1029, July 2023.

[20] Juhn Atsushi Wada. A new method for the determination of the side of cerebral speech dominance. a preliminary report of the intra-carotid injection of sodium amytal in man. *Igaku to Seibutsugaki*, 14:221–222, 1949.

[21] Charles M Epstein, Kimford J Meador, David W Loring, Randall J Wright, Joseph D Weissman, Scott Sheppard, James J Lah, Frank Puhalovich, Luis Gaitan, and Kent R Davey. Localization and characterization of speech arrest during transcranial magnetic stimulation. *Clinical Neurophysiology*, 110(6):1073–1079, June 1999.

[22] J. Rösler, B. Niraula, V. Strack, A. Zdunczyk, S. Schilt, P. Savolainen, P. Lioumis, J. Mäkelä, P. Vajkoczy, D. Frey, and T. Picht. Language mapping in healthy volunteers and brain tumor patients with a novel navigated tms system: Evidence of tumor-induced plasticity. *Clinical Neurophysiology*, 125(3):526–536, 2014.

[23] Wanying Zhao, Yanchang Li, and Yinjuan Du. Tms reveals dynamic interaction between inferior frontal gyrus and posterior middle temporal gyrus in gesture-speech semantic integration. *The Journal of Neuroscience*, 41:10356 – 10364, 2021.

[24] R. Töpper, F. M. Mottaghy, M. Brügmann, J. Noth, and W. Huber. Facilitation of picture naming by focal transcranial magnetic stimulation of wernicke's area. *Experimental Brain Research*, 121(4):371–378, August 1998.

[25] Alvaro Pascual-Leone, Jordan Grafman, and Mark Hallett. Modulation of cortical motor output maps during development of implicit and explicit knowledge. *Science*, 263(5151):1287–1289, 1994.

[26] Bradley R. Postle, Fabio Ferrarelli, Massihullah Hamidi, Eva Feredoes, Marcello Massimini, Michael Peterson, Andrew Alexander, and Giulio Tononi. Repetitive transcranial magnetic stimulation dissociates working memory manipulation from retention functions in the prefrontal, but not posterior parietal, cortex. *Journal of Cognitive Neuroscience*, 18(10):1712–1722, October 2006.

[27] Joseph Classen, Joachim Liepert, Steven P. Wise, Mark Hallett, and Leonardo G. Cohen. Rapid plasticity of human cortical movement representation induced by practice. *Journal of Neurophysiology*, 79(2):1117–1123, February 1998.

[28] Ying-Zu Huang, Mark J. Edwards, Elisabeth Rounis, Kailash P. Bhatia, and John C. Rothwell. Theta burst stimulation of the human motor cortex. *Neuron*, 45(2):201–206, 2005.

[29] Ali Jannati, Lindsay M. Oberman, Alexander Rotenberg, and Alvaro Pascual-Leone. Assessing the mechanisms of brain plasticity by transcranial magnetic stimulation. *Neuropsychopharmacology*, 48(1):191–208, October 2022.

[30] American Psychiatric Association. *Diagnostic and Statistical Manual of Mental Disorders*. American Psychiatric Association, fifth edition edition, May 2013.

[31] Mark S. George, Eric M. Wassermann, Wendol A. Williams, Ann Callahan, Terence A. Ketter, Peter Basser, Mark Hallett, and Robert M. Post. Daily repetitive transcranial magnetic stimulation (rtms) improves mood in depression. *NeuroReport*, 6(14):1853–1856, October 1995.

[32] Colm G. Connolly, Jing Wu, Tiffany C. Ho, Fumiko Hoeft, Owen Wolkowitz, Stuart Eisendrath, Guido Frank, Robert Hendren, Jeffrey E. Max, Martin P. Paulus, Susan F. Tapert, Dipavo Banerjee, Alan N. Simmons, and Tony T. Yang. Resting-state functional connectivity of subgenual anterior cingulate cortex in depressed adolescents. *Biological Psychiatry*, 74(12):898–907, 2013. Cortico-limbic Connectivity and Mood Disorders.

[33] Vinh Tan, Jerrold Jeyachandra, Ruiyang Ge, Erin W. Dickie, Elizabeth Gregory, Tamara Vanderwal, Fidel Vila-Rodriguez, and Colin Hawco. Subgenual cingulate connectivity as a treatment predictor during low-frequency right dorsolateral prefrontal rtms: A concurrent tms-fmri study. *Brain Stimulation*, 16(4):1165–1172, 2023.

[34] Michael D. Fox, Mark A. Halko, Mark C. Eldaief, and Alvaro Pascual-Leone. Measuring and manipulating brain connectivity with resting state functional connectivity magnetic resonance imaging (fcmri) and transcranial magnetic stimulation (tms). *NeuroImage*, 62(4):2232–2243, 2012. Connectivity.

[35] Petya Vicheva, Curtis Osborne, Sandro M. Krieg, Rezvan Ahmadi, and Paul Shotbolt. Transcranial magnetic stimulation for obsessive-compulsive disorder and post-traumatic stress disorder: A comprehensive systematic review and analysis of therapeutic benefits, cortical targets, and psychopathophysiological mechanisms. *Progress in Neuro-Psychopharmacology and Biological Psychiatry*, 136:111147, 2025.

[36] Robert S. Fisher, Carlos Acevedo, Alexis Arzimanoglou, Alicia Bogacz, J. Helen Cross, Christian E. Elger, Jerome Engel Jr, Lars Forsgren, Jacqueline A. French, Mike Glynn, Dale C. Hesdorffer, B.I. Lee, Gary W. Mathern, Solomon L. Moshé, Emilio Perucca, Ingrid E. Scheffer, Torbjörn Tomson, Masako Watanabe, and Samuel Wiebe. Ilae official report: A practical clinical definition of epilepsy. *Epilepsia*, 55(4):475–482, 2014.

[37] P. C. Lauterbur. Image formation by induced local interactions: Examples employing nuclear magnetic resonance. *Nature*, 242(5394):190–191, March 1973.

[38] Scott A. Huettel, Allen W. Song, and Gregory McCarthy. *Functional Magnetic Resonance Imaging*. Sinauer Associates, Sunderland, MA, 3rd edition, 2014.

[39] Per E. Roland. *Brain activation*. Wiley-Liss, New York, 1993 - 1993.

[40] Richard B. Buxton and Lawrence R. Frank. A model for the coupling between cerebral blood flow and oxygen metabolism during neural stimulation. *Journal of Cerebral Blood Flow & Metabolism*, 17(1):64–72, January 1997.

[41] Richard B. Buxton, Eric C. Wong, and Lawrence R. Frank. Dynamics of blood flow and oxygenation changes during brain activation: The balloon model. *Magnetic Resonance in Medicine*, 39(6):855–864, June 1998.

[42] S Ogawa, T M Lee, A R Kay, and D W Tank. Brain magnetic resonance imaging with contrast dependent on blood oxygenation. *Proceedings of the National Academy of Sciences*, 87(24):9868–9872, December 1990.

[43] Peter A. Bandettini, Eric C. Wong, R. Scott Hinks, Ronald S. Tikofsky, and James S. Hyde. Time course epi of human brain function during task activation. *Magnetic Resonance in Medicine*, 25(2):390–397, June 1992.

[44] K K Kwong, J W Belliveau, D A Chesler, I E Goldberg, R M Weisskoff, B P Poncelet, D N Kennedy, B E Hoppel, M S Cohen, and R Turner. Dynamic magnetic resonance imaging of human brain activity during primary sensory stimulation. *Proceedings of the National Academy of Sciences*, 89(12):5675–5679, June 1992.

[45] S. Ogawa, R.S. Menon, D.W. Tank, S.G. Kim, H. Merkle, J.M. Ellermann, and K. Ugurbil. Functional brain mapping by blood oxygenation level-dependent contrast magnetic resonance imaging. a comparison of signal characteristics with a biophysical model. *Biophysical Journal*, 64(3):803–812, March 1993.

[46] Keith R. Thulborn, John C. Waterton, Paul M. Matthews, and George K. Radda. Oxygenation dependence of the transverse relaxation time of water protons in whole blood at high field. *Biochimica et Biophysica Acta (BBA) - General Subjects*, 714(2):265–270, February 1982.

[47] D. Rangaprakash, Guo-Rong Wu, Daniele Marinazzo, Xiaoping Hu, and Gopikrishna Deshpande. Hemodynamic response function (hrf) variability confounds resting-state fmri functional connectivity. *Magnetic Resonance in Medicine*, 80(4):1697–1713, April 2018.

[48] Bharat Biswal, F. Zerrin Yetkin, Victor M. Haughton, and James S. Hyde. Functional connectivity in the motor cortex of resting human brain using echo-planar mri. *Magnetic Resonance in Medicine*, 34(4):537–541, October 1995.

[49] Michael D. Fox and Marcus E. Raichle. Spontaneous fluctuations in brain activity observed with functional magnetic resonance imaging. *Nature Reviews Neuroscience*, 8(9):700–711, September 2007.

[50] Marcus E. Raichle, Ann Mary MacLeod, Abraham Z. Snyder, William J. Powers, Debra A. Gusnard, and Gordon L. Shulman. A default mode of brain function. *Proceedings of the National Academy of Sciences*, 98(2):676–682, January 2001.

[51] Yuki Mizutani-Tiebel, Martin Tik, Kai-Yen Chang, Frank Padberg, Aldo Soldini, Zane Wilkinson, Cui Ci Voon, Lucia Bulubas, Christian Windischberger, and Daniel Keeser. Concurrent tms-fmri: Technical challenges, developments, and overview of previous studies. *Frontiers in Psychiatry*, Volume 13 - 2022, 2022.

[52] Martin J. Ryan, Robert K. Erickson, David N. Levin, Charles A. Pelizzari, R. Loch Macdonald, and George J. Dohrmann. Frameless stereotaxy with real-time tracking of patient head movement and retrospective patient—image registration. *Journal of Neurosurgery*, 85(2):287–292, August 1996.

[53] Richard I. Hartley and Peter Sturm. Triangulation. *Comput. Vis. Image Underst.*, 68(2):146–157, November 1997.

[54] J M Fitzpatrick. The role of registration in accurate surgical guidance. *Proceedings of the Institution of Mechanical Engineers, Part H: Journal of Engineering in Medicine*, 224(5):607–622, September 2009.

[55] Michael Woletz, Martin Tik, Maxim Zaitsev, Sarah Großhagauer, Maria Vasileiadi, and Christian Windischberger. Automated subject registration for neuro-navigated brain-stimulation. *Brain Stimulation*, 16(1):345–346, 2023.

[56] Sven Bestmann, Jürgen Baudewig, Hartwig R. Siebner, John C. Rothwell, and Jens Frahm. Bold mri responses to repetitive tms over human dorsal premotor cortex. *NeuroImage*, 28(1):22–29, October 2005.

[57] J. Andoh, E. Artiges, C. Pallier, D. Riviere, J.-F. Mangin, M.-L. Paillere-Martinot, and J.-L. Martinot. Priming frequencies of transcranial magnetic stimulation over wernicke's area modulate word detection. *Cerebral Cortex*, 18(1):210–216, May 2007.

[58] Molly S. Hermiller, Yu Fen Chen, Todd B. Parrish, and Joel L. Voss. Evidence for immediate enhancement of hippocampal memory encoding by network-targeted theta-burst stimulation during concurrent fmri. *The Journal of Neuroscience*, 40(37):7155–7168, August 2020.

[59] Erol Başar, Canan Başar-Eroglu, Sirel Karakaş, and Martin Schürmann. Gamma, alpha, delta, and theta oscillations govern cognitive processes. *International Journal of Psychophysiology*, 39(2):241–248, 2001.

[60] Judith C. Peters, Joel Reithler, Tom A. de Graaf, Teresa Schuhmann, Rainer Goebel, and Alexander T. Sack. Concurrent human tms-eeg-fmri enables monitoring of oscillatory brain state-dependent gating of cortico-subcortical network activity. *Communications Biology*, 3(1), January 2020.

[61] M. Tik, M. Woletz, A.-L. Schuler, M. Vasileiadi, R.F.H. Cash, A. Zalesky, C. Lamm, and C. Windischberger. Acute tms/fmri response explains offline tms network effects – an interleaved tms-fmri study. *NeuroImage*, 267:119833, February 2023.

[62] Martin Tik, Maria Vasileiadi, Michael Woletz, David Linhardt, Anna-Lisa Schuler, Nolan Williams, and Christian Windischberger. Concurrent tms/fmri reveals individual dlpfc dose-response pattern. *NeuroImage*, 282:120394, November 2023.

[63] Sarah Grosshagauer, Michael Woletz, Maria Vasileiadi, David Linhardt, Lena Nohava, Anna-Lisa Schuler, Christian Windischberger, Nolan Williams, and Martin Tik. Chronometric tms-fmri of personalized left dorsolateral prefrontal target reveals state-dependency of subgenual anterior cingulate cortex effects. *Molecular Psychiatry*, 29(9):2678–2688, March 2024.

[64] Ruiyang Ge, Afifa Humaira, Elizabeth Gregory, Golnoush Alamian, Erin L. MacMillan, Laura Barlow, Rebecca Todd, Sean Nestor, Sophia Frangou, and Fidel Vila-Rodriguez. Predictive value of acute neuroplastic response to rtms in treatment outcome in depression: A concurrent tms-fmri trial. *American Journal of Psychiatry*, 179(7):500–508, July 2022.

[65] Allen Newell and Herbert A. Simon. Computer science as empirical inquiry: symbols and search. *Commun. ACM*, 19(3):113–126, March 1976.

[66] Marvin Minsky. Steps toward artificial intelligence. *Proceedings of the IRE*, 49(1):8–30, 1961.

[67] Ulric Neisser. *Cognitive Psychology*. Appleton-Century-Crofts, 1967.

[68] Juha Silvanto, Neil Muggleton, and Vincent Walsh. State-dependency in brain stimulation studies of perception and cognition. *Trends in Cognitive Sciences*, 12(12):447–454, 2008.

[69] Andy Clark. Whatever next? predictive brains, situated agents, and the future of cognitive science. *Behavioral and Brain Sciences*, 36(3):181–204, May 2013.

[70] Jakob Hohwy. *The Predictive Mind*. Oxford University Press, November 2013.

[71] Csaba Orban, Ru Kong, Jingwei Li, Michael W. L. Chee, and B. T. Thomas Yeo. Time of day is associated with paradoxical reductions in global signal fluctuation and functional connectivity. *PLOS Biology*, 18(2):e3000602, February 2020.

[72] Gonçalo Cotovio, Albino J. Oliveira-Maia, Carter Paul, Francisco Faro Viana, Daniel Rodrigues da Silva, Carolina Seybert, Adam P. Stern, Alvaro Pascual-Leone, and Daniel Z. Press. Day-to-day variability in motor threshold during rtms treatment for depression: Clinical implications. *Brain Stimulation*, 14(5):1118–1125, September 2021.

[73] P.M. Rossini, D. Burke, R. Chen, L.G. Cohen, Z. Daskalakis, R. Di Iorio, V. Di Lazzaro, F. Ferreri, P.B. Fitzgerald, M.S. George, M. Hallett, J.P. Lefaucheur, B. Langguth, H. Matsumoto, C. Miniussi, M.A. Nitsche, A. Pascual-Leone, W. Paulus, S. Rossi, J.C. Rothwell, H.R. Siebner, Y. Ugawa, V. Walsh, and U. Ziemann. Non-invasive electrical and magnetic stimulation of the brain, spinal cord, roots and peripheral nerves: Basic principles and procedures for routine clinical and research application. an updated report from an i.f.c.n. committee. *Clinical Neurophysiology*, 126(6):1071–1107, 2015.

[74] Lucia I. Navarro de Lara, Christian Windischberger, Andre Kuehne, Michael Woletz, Jürgen Sieg, Sven Bestmann, Nikolaus Weiskopf, Bernhard Strasser, Ewald Moser, and Elmar Laistler. A novel coil array for combined tms/fmri experiments at 3 t. *Magnetic Resonance in Medicine*, 74(5):1492–1501, November 2014.

[75] Luis J. Gomez, Moritz Dannhauer, and Angel V. Peterchev. Fast computational optimization of tms coil placement for individualized electric field targeting. *NeuroImage*, 228:117696, 2021.

[76] Mark G. Stokes, Christopher D. Chambers, Ian C. Gould, Therese English, Elizabeth McNaught, Odette McDonald, and Jason B. Mattingley. Distance-adjusted motor threshold for transcranial magnetic stimulation. *Clinical Neurophysiology*, 118(7):1617–1625, July 2007.

[77] Max Koehler, Thomas Kammer, and Stefan Goetz. How coil misalignment and mispositioning in transcranial magnetic stimulation affect the stimulation strength at the target. *Clinical Neurophysiology*, 162:159–161, June 2024.

[78] Arno M Janssen, Thom F Oostendorp, and Dick F Stegeman. The coil orientation dependency of the electric field induced by tms for m1 and other brain areas. *Journal of NeuroEngineering and Rehabilitation*, 12(1), May 2015.

[79] Andriy Fedorov, Reinhard Beichel, Jayashree Kalpathy-Cramer, Julien Finet, Jean-Christophe Fillion-Robin, Sonia Pujol, Christian Bauer, Dylan Jennings, Fiona M. Fennessy, Milan Sonka, John Buatti, Stephen R. Aylward, James V. Miller, Steve Pieper, and Ron Kikinis. 3d slicer as an image computing platform for the quantitative imaging network. *Magnetic Resonance Imaging*, 30(9):1323–1341, November 2012.

[80] Oscar Esteban, Christopher Markiewicz, Ross W Blair, Craig Moodie, Ayse Ilkay Isik, Asier Erramuzpe Aliaga, James Kent, Mathias Goncalves, Elizabeth DuPre,

Madeleine Snyder, Hiroyuki Oya, Satrajit Ghosh, Jessey Wright, Joke Durnez, Russell Poldrack, and Krzysztof Jacek Gorgolewski. fMRIPrep: a robust preprocessing pipeline for functional MRI. *Nature Methods*, 16:111–116, 2019.

[81] Oscar Esteban, Ross Blair, Christopher J. Markiewicz, Shoshana L. Berleant, Craig Moodie, Feilong Ma, Ayse Ilkay Isik, Asier Erramuzpe, Mathias Kent, James D. andGoncalves, Elizabeth DuPre, Kevin R. Sitek, Daniel E. P. Gomez, Daniel J. Lurie, Zhifang Ye, Russell A. Poldrack, and Krzysztof J. Gorgolewski. fmriprep. *Software*, 2018.

[82] K. Gorgolewski, C. D. Burns, C. Madison, D. Clark, Y. O. Halchenko, M. L. Waskom, and S. Ghosh. Nipype: a flexible, lightweight and extensible neuroimaging data processing framework in python. *Frontiers in Neuroinformatics*, 5:13, 2011.

[83] Krzysztof J. Gorgolewski, Oscar Esteban, Christopher J. Markiewicz, Erik Ziegler, David Gage Ellis, Michael Philipp Notter, Dorota Jarecka, Hans Johnson, Christopher Burns, Alexandre Manhães-Savio, Carlo Hamalainen, Benjamin Yvernault, Taylor Salo, Kesshi Jordan, Mathias Goncalves, Michael Waskom, Daniel Clark, Jason Wong, Fred Loney, Marc Modat, Blake E Dewey, Cindee Madison, Matteo Visconti di Oleggio Castello, Michael G. Clark, Michael Dayan, Dav Clark, Anisha Keshavan, Basile Pinsard, Alexandre Gramfort, Shoshana Berleant, Dylan M. Nielson, Salma Bougacha, Gael Varoquaux, Ben Cipollini, Ross Markello, Ariel Rokem, Brendan Moloney, Yaroslav O. Halchenko, Demian Wassermann, Michael Hanke, Christian Horea, Jakub Kaczmarzyk, Gilles de Hollander, Elizabeth DuPre, Ashley Gillman, David Mordom, Colin Buchanan, Rosalia Tungaraza, Wolfgang M. Pauli, Shariq Iqbal, Sharad Sikka, Matteo Mancini, Yannick Schwartz, Ian B. Malone, Mathieu Dubois, Caroline Frohlich, David Welch, Jessica Forbes, James Kent, Aimi Watanabe, Chad Cumba, Julia M. Huntenburg, Erik Kastman, B. Nolan Nichols, Arman Eshaghi, Daniel Ginsburg, Alexander Schaefer, Benjamin Acland, Steven Giavasis, Jens Kleesiek, Drew Erickson, René Küttner, Christian Haselgrove, Carlos Correa, Ali Ghayoor, Franz Liem, Jarrod Millman, Daniel Haehn, Jeff Lai, Dale Zhou, Ross Blair, Tristan Glatard, Mandy Renfro, Siqi Liu, Ari E. Kahn, Fernando Pérez-García, William Triplett, Leonie Lampe, Jörg Stadler, Xiang-Zhen Kong, Michael Hallquist, Andrey Chetverikov, John Salvatore, Anne Park, Russell Poldrack, R. Cameron Craddock, Souheil Inati, Oliver Hinds, Gavin Cooper, L. Nathan Perkins, Ana Marina, Aaron Mattfeld, Maxime Noel, Lukas Snoek, K Matsubara, Brian Cheung, Simon Rothmei, Sebastian Urchs, Joke Durnez, Fred Mertz, Daniel Geisler, Andrew Floren, Stephan Gerhard, Paul Sharp, Miguel Molina-Romero, Alejandro Weinstein, William Broderick, Victor Saase, Sami Kristian Andberg, Robbert Harms, Kai Schlamp, Jaime Arias, Dimitri Papadopoulos Orfanos, Claire Tarbert, Arielle Tambini, Alejandro De La Vega, Thomas Nickson, Matthew Brett, Marcel Falkiewicz, Kornelius Podranski, Janosch Linkersdörfer, Guillaume Flandin, Eduard Ort, Dmitry Shachnev, Daniel McNamee, Andrew Davison, Jan Varada, Isaac Schwabacher, John Pellman, Martin Perez-Guevara, Ranjeet Khanuja, Nicolas Pannetier, Conor McDermottroe, and Satrajit Ghosh. Nipype. *Software*, 2018.

[84] Jesper L.R. Andersson, Stefan Skare, and John Ashburner. How to correct susceptibility distortions in spin-echo echo-planar images: application to diffusion tensor imaging. *NeuroImage*, 20(2):870–888, 2003.

[85] Anders M. Dale, Bruce Fischl, and Martin I. Sereno. Cortical surface-based analysis: I. segmentation and surface reconstruction. *NeuroImage*, 9(2):179–194, 1999.

[86] Arno Klein, Satrajit S. Ghosh, Forrest S. Bao, Joachim Giard, Yrjö Häme, Eliezer Stavsky, Noah Lee, Brian Rossa, Martin Reuter, Elias Chaibub Neto, and Anisha Keshavan. Mindboggling morphometry of human brains. *PLOS Computational Biology*, 13(2):e1005350, 2017.

[87] Mark Jenkinson and Stephen Smith. A global optimisation method for robust affine registration of brain images. *Medical Image Analysis*, 5(2):143–156, 2001.

[88] Douglas N Greve and Bruce Fischl. Accurate and robust brain image alignment using boundary-based registration. *NeuroImage*, 48(1):63–72, 2009.

[89] Jonathan D. Power, Anish Mitra, Timothy O. Laumann, Abraham Z. Snyder, Bradley L. Schlaggar, and Steven E. Petersen. Methods to detect, characterize, and remove motion artifact in resting state fmri. *NeuroImage*, 84(Supplement C):320–341, 2014.

[90] Yashar Behzadi, Khaled Restom, Joy Liau, and Thomas T. Liu. A component based noise correction method (CompCor) for BOLD and perfusion based fmri. *NeuroImage*, 37(1):90–101, 2007.

[91] Theodore D. Satterthwaite, Mark A. Elliott, Raphael T. Gerraty, Kosha Ruparel, James Loughead, Monica E. Calkins, Simon B. Eickhoff, Hakon Hakonarson, Ruben C. Gur, Raquel E. Gur, and Daniel H. Wolf. An improved framework for confound regression and filtering for control of motion artifact in the preprocessing of resting-state functional connectivity data. *NeuroImage*, 64(1):240–256, 2013.

[92] Rémi Patriat, Richard C. Reynolds, and Rasmus M. Birn. An improved model of motion-related signal changes in fMRI. *NeuroImage*, 144, Part A:74–82, January 2017.

[93] Alexandre Abraham, Fabian Pedregosa, Michael Eickenberg, Philippe Gervais, Andreas Mueller, Jean Kossaifi, Alexandre Gramfort, Bertrand Thirion, and Gael Varoquaux. Machine learning for neuroimaging with scikit-learn. *Frontiers in Neuroinformatics*, 8, 2014.

[94] Nilearn contributors. nilearn.

[95] Alexander Schaefer, Ru Kong, Evan M Gordon, Timothy O Laumann, Xi-Nian Zuo, Avram J Holmes, Simon B Eickhoff, and B T Thomas Yeo. Local-global parcellation

of the human cerebral cortex from intrinsic functional connectivity mri. *Cerebral Cortex*, 28(9):3095–3114, July 2017.

[96] B. T. Thomas Yeo, Fenna M. Krienen, Jorge Sepulcre, Mert R. Sabuncu, Danial Lashkari, Marisa Hollinshead, Joshua L. Roffman, Jordan W. Smoller, Lilla Zöllei, Jonathan R. Polimeni, Bruce Fischl, Hesheng Liu, and Randy L. Buckner. The organization of the human cerebral cortex estimated by intrinsic functional connectivity. *Journal of Neurophysiology*, 106(3):1125–1165, 2011. PMID: 21653723.

[97] Dennis J.L.G. Schutter and Jack van Honk. A standardized motor threshold estimation procedure for transcranial magnetic stimulation research. *The Journal of ECT*, 22(3):176–178, September 2006.

[98] John Temesi, Mathieu Gruet, Thomas Rupp, Samuel Verges, and Guillaume Y Millet. Resting and active motor thresholds versus stimulus–response curves to determine transcranial magnetic stimulation intensity in quadriceps femoris. *Journal of NeuroEngineering and Rehabilitation*, 11(1), March 2014.

[99] Aino E Nieminen, Jaakko O Nieminen, Matti Stenroos, Pavel Novikov, Maria Nazarova, Selja Vaalto, Vadim Nikulin, and Risto J Ilmoniemi. Accuracy and precision of navigated transcranial magnetic stimulation. *Journal of Neural Engineering*, 19(6):066037, December 2022.

[100] Robin F.H. Cash, Anne Weigand, Andrew Zalesky, Shan H. Siddiqi, Jonathan Downar, Paul B. Fitzgerald, and Michael D. Fox. Using brain imaging to improve spatial targeting of transcranial magnetic stimulation for depression. *Biological Psychiatry*, 90(10):689–700, 2021. Neurostimulation for Psychiatric Disorders.

[101] Michael D. Fox, Hesheng Liu, and Alvaro Pascual-Leone. Identification of reproducible individualized targets for treatment of depression with tms based on intrinsic connectivity. *NeuroImage*, 66:151–160, 2013.

[102] Anne Weigand, Andreas Horn, Ruth Caballero, Danielle Cooke, Adam P. Stern, Stephan F. Taylor, Daniel Press, Alvaro Pascual-Leone, and Michael D. Fox. Prospective validation that subgenual connectivity predicts antidepressant efficacy of transcranial magnetic stimulation sites. *Biological Psychiatry*, 84(1):28–37, July 2018.

[103] N. Tzourio-Mazoyer, B. Landeau, D. Papathanassiou, F. Crivello, O. Etard, N. Delcroix, B. Mazoyer, and M. Joliot. Automated anatomical labeling of activations in spm using a macroscopic anatomical parcellation of the mni mri single-subject brain. *NeuroImage*, 15(1):273–289, 2002.

A. Appendix

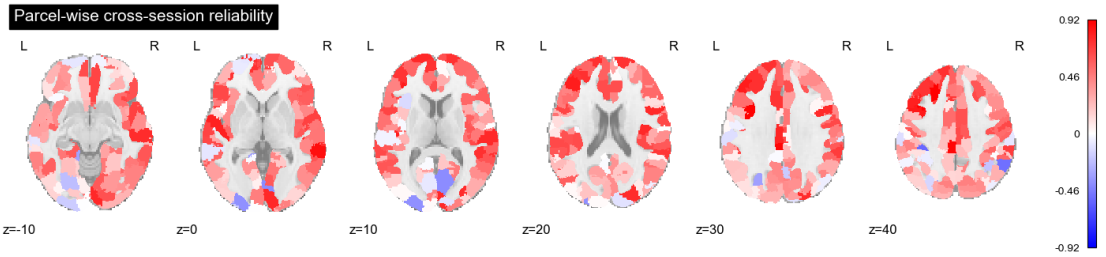

Figure A.1.: Correlation's of specific brain ROI's based on the Schaefer atlases [95]. The coloration of the parcel corresponds to its' respective correlation between ses-02 and ses-03 across subjects.

Figure A.1 shows relevant parcel specific correlations between ses-02 and ses-03 across subjects adjusted to fit onto the MNI template brain. The red parcels represent highly correlated areas and the blue hues represent the inversely correlated areas. High correlations can be seen in the frontal cortical parts as well as Somatomotor areas.

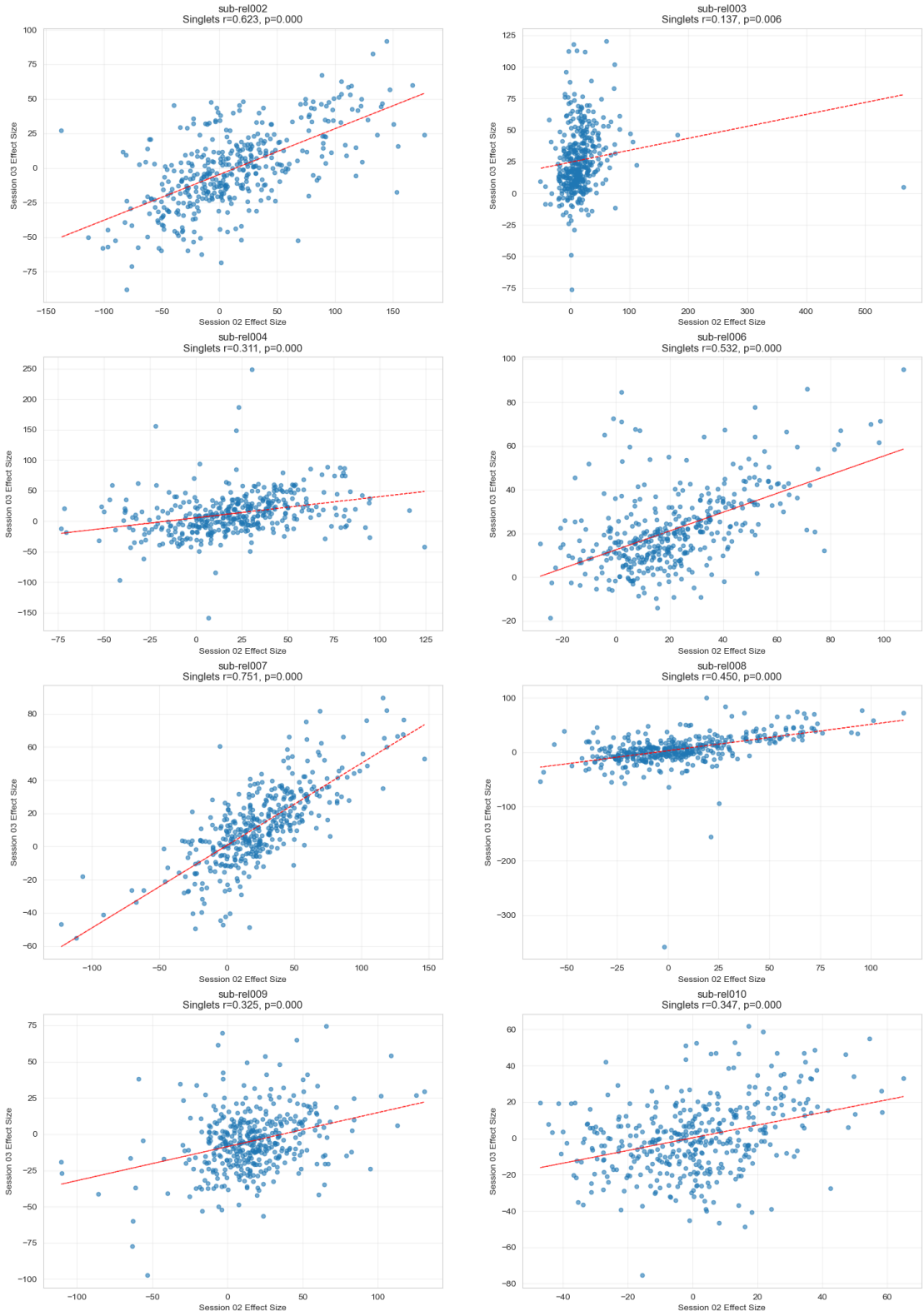

Figure A.2.: Parcel-wise correspondence of singlet-evoked BOLD effect sizes across sessions for all participants. Each point represents a cortical parcel, plotting its effect size in ses-02 against ses-03. The red regression line illustrates the correlation between sessions.

Figure A.3.: Parcel-wise correspondence of triplet-evoked BOLD effect sizes across sessions for all participants. Each point represents a cortical parcel, plotting its effect size in ses-02 against ses-03. The red regression line illustrates the correlation between sessions.

Subject	Protocol	correlation	p
sub-rel002	singlets	0.623	0.000
	triplets	0.768	0.000
sub-rel003	singlets	0.137	0.006
	triplets	0.571	0.000
sub-rel004	singlets	0.311	0.000
	triplets	0.508	0.000
sub-rel006	singlets	0.532	0.000
	triplets	0.422	0.000
sub-rel007	singlets	0.751	0.000
	triplets	0.544	0.000
sub-rel008	singlets	0.450	0.000
	triplets	0.610	0.000
sub-rel009	singlets	0.325	0.000
	triplets	0.395	0.000
sub-rel010	singlets	0.347	0.000
	triplets	0.586	0.000

Table A.1.: Correlation coefficients and p-values for within-subject cross-session consistency across singlets and triplets.